Economic Geology, v. 117, no. 6, pp. 1387–1403

GEOCHRONOLOGY OF Sn MINERALIZATION IN MYANMAR: METALLOGENIC IMPLICATIONS

Wei Mao,[1] Hong Zhong,[1,2,†] Jiehua Yang,[1] Liang Liu,[1] Yazhou Fu,[1] Xingchun Zhang,[1] Yanwen Tang,[1] Jie Li,[3] Le Zhang,[3] Kyaing Sein,[4] Soe Myint Aung,[4] Saw Mu Tha Lay Paw,[5] and Saw Hpa Doh[5]

[1]*State Key Laboratory of Ore Deposit Geochemistry, Institute of Geochemistry, Chinese Academy of Sciences, Guiyang 550081, China*

[2]*University of Chinese Academy of Sciences, Beijing 100049, China*

[3]*State Key Laboratory of Isotope Geochemistry, Guangzhou Institute of Geochemistry, Chinese Academy of Sciences, Guangzhou 510640, China*

[4]*Myanmar Geosciences Society, Yangon 11041, Myanmar*

[5]*Kamayut Township, Yangon 11041, Myanmar*

Abstract

Myanmar, the third largest global tin supplier, is an important component of the Southeast Asian tin province. We have conducted laser ablation-inductively coupled plasma-mass spectrometry U-Pb dating of cassiterite, wolframite, and zircon and Re-Os dating of molybdenite from six primary and two placer Sn deposits in Myanmar. A combination of our geochronological data with previous studies revealed that three episodes of Sn mineralization in the Western tin belt of Southeast Asia formed during the closure of multiple Tethys oceans, namely the Late Triassic (~218 Ma) mineralization in a collisional setting after closure of the Paleo-Tethys, the Early Cretaceous (~124–107 Ma) mineralization during subduction of the Meso-Tethys, and the Late Cretaceous to Eocene (~90–42 Ma) mineralization related to the Neo-Tethys subduction. Recurrent Sn mineralization is recorded not only in the Western tin belt but also in the Central and Eastern tin belts in Southeast Asia. Compilation of currently available cassiterite U-Pb ages from all over the world revealed that durations of regional Sn mineralization events are typically in the range of ~5–30 m.y., whereas the Neo-Tethys subduction in Southeast Asia generated prolonged Sn mineralization lasting up to ~50 m.y. The Southeast Asian tin province, as a whole, has the longest cumulative episodes of mineralization, compared to other Sn provinces. The Sn mineralization ceased in the late Eocene when the tectonic setting changed from Neo-Tethys subduction to dextral motion along a series of strike-slip faults and extrusion of the Indochina block in Southeast Asia.

Introduction

Tin (Sn) was one of the first metals used by humankind, and it is still playing a critical role in modern industry (Schulz et al., 2017). The abundance of Sn in the bulk continental crust is only ~1.7 ppm (Rudnick and Gao, 2014), but this metal can form large metallogenic provinces with great economic significance (Taylor, 1979; Lehmann, 1990). For example, ~85% of the historical tin production was mined from the Southeast Asian (40~45%), South China (20%), Central Andean (14%), and Cornwall (7%) tin provinces (Lehmann, 2021). These tin provinces still provide ~85% of the current global tin production and two-thirds of the tin reserves (USGS, 2020). The Southeast Asian tin province is a 3,500-km-long belt that extends from western Yunnan through Myanmar and Thailand to Peninsular Malaysia and the Indonesian tin islands (Mitchell, 1977, 1979, 2018; Beckinsale, 1979; Schwartz et al., 1995). Myanmar is the third global tin supplier after China and Indonesia, accounting for ~17% of the world's annual production in recent years (Lehmann, 2021). Scientific research on Sn mineralization in Myanmar has been conducted since the 1930s, with respect to the geologic setting, magma evolution, mineralization age, and ore-forming mechanism (Chhibber, 1934; Clegg, 1944a, b; Mitchell, 1977, 1979, 1986; Hutchison and Taylor, 1978; Bender, 1983; Gardiner et al., 2014a, b, 2015a, 2016a, 2017, 2018; Jiang et al., 2017, 2019; Zaw, 2017; Li, J.X., et al., 2018, 2019; Mao et al., 2020; Mitchell et al., 2021; Myint et al., 2021).

Ages of Sn mineralization are critical to linking the formation of resources to tectonic and magmatic evolution (e.g., Mitchell et al., 2012; Mao et al., 2013; Romer and Kroner, 2016; Zhang et al., 2017a). Previous geochronology studies in Myanmar mainly focused on ore-forming granites with conventional whole-rock/mineral Rb-Sr, Sm-Nd, K/Ar-Ar, and zircon U-Pb methods (e.g., Lehmann and Mahawat, 1989; Cobbing et al., 1992). However, the whole-rock and mineral Rb-Sr, Sm-Nd, and K/Ar-Ar systems have relatively low closure temperature and are apt to be disturbed by later thermal events (Romer et al., 2007; Ganguly and Tirone, 2009). Elevated U contents in zircon from highly fractionated granite may cause α-recoil damage, which disturbs the U-Pb system (Davis and Krogh, 2000; Romer, 2003). In contrast, ore minerals like cassiterite and wolframite may incorporate sufficiently high contents of U and low amounts of Pb, making them suitable for U-Pb dating (Gulson and Jones, 1992; Yuan et al., 2008; Tang et al., 2020). The U-Pb system in cassiterite and wolframite has closure temperatures higher than those of Sn and W mineralization and therefore may remain stable during later hydrothermal events (Zhang et al., 2011; Yang, M., et al., 2020). In this study, we conducted in situ U-Pb dating of cassiterite and wolframite from six primary Sn deposits and two placer deposits in Myanmar, as well as zircon U-Pb dating and molybdenite Re-Os dating, and we

†Corresponding author: e-mail, zhonghong@vip.gyig.ac.cn

ISSN 0361-0128; doi:10.5382/econgeo.4927; 17 p.
Digital appendices are available in the online Supplements section.

Submitted: July 28, 2021 / Accepted: October 27, 2021

discuss the regional and global geologic significance of these geochronological results.

Geologic Background

Regional geologic setting

A series of tectonic boundaries were formed in Southeast Asia during the closure of multiple Tethys oceans and back-arc basins from the Permian to the Cenozoic (Garson and Mitchell, 1970; Mitchell, 1977, 1979, 1986; Mitchell and Garson, 1981; Metcalfe, 1984, 1996, 2011, 2013; Cobbing et al., 1986; Sone and Metcalfe, 2008; Mitchell et al., 2015; Cong et al., 2021). The Paleo-Tethys represented by the Longmu Co-Shuanghu and Changning-Menglian sutures in China were connected to the Chiang Rai suture in Thailand and the Bentong-Raub suture in Malaysia (Fig. 1; Metcalfe, 2013, 2021). However, the southward continuation of the Bangong-Nujiang suture of the Meso-Tethys and Yarlung-Tsangpo suture of the Neo-Tethys from China to Myanmar remains controversial (Mitchell et al., 2015, 2021; Liu et al., 2016a, b; Metcalfe, 2021). The Kalaymyo and Myitkyina ophiolites were proposed to belong to a single suture that connected to the Yarlung-Tsangpo suture in Tibet and was displaced by the post-early Oligocene dextral Sagaing fault (Sengör et al., 1988; Mitchell, 1993). However, geochronology of ophiolites by Liu et al. (2016a) suggested that the Myitkyina suture is the southern continuation of the Bangong-Nujiang suture, and the Kalaymyo suture connects to the Yarlung-Tsangpo suture. Metcalfe (1984, 1996) inferred that the Shan boundary and the Myitkyina suture represent the Meso-Tethys in Myanmar. The Medial Myanmar zone was postulated to be a cryptic suture (Fig. 1; Mitchell et al., 2015; Ridd, 2016) but reinterpreted to be a dextral shear zone (Ridd, 2017; Ridd et al., 2019) or a narrow basin between the Myittha Chaung extensional fault and the Late Cretaceous Pan Laung fault (Mitchell et al., 2021).

Tin mineralization in the Southeast Asian tin province was divided into three main belts, based on the spatial distribution, tectonic setting, and mineralization ages (Fig. 1; Mitchell, 1977, 1979, 2018; Mitchell and Garson, 1981; Cobbing et al., 1986; Schwartz et al., 1995; Sone and Metcalfe, 2008). The Eastern tin belt, mainly distributed in the eastern Peninsular Malaysia, was formed during the subduction of the Paleo-Tethys from the Permian to the Triassic (Mitchell, 1977; Cobbing et al., 1986; Charusiri et al., 1993; Metcalfe, 1996). The Central tin belt hosts productive segments in the Indonesia tin islands and western Peninsular Malaysia and was formed after closure of the Paleo-Tethys in the Late Triassic (Mitchell, 1977; Beckinsale, 1979; Mitchell and Garson, 1981; Searle et al., 2012; Ng et al., 2015). The Western tin belt extends from the western margin of the Shan states through Peninsular Myanmar to the Phuket Islands in Thailand (Mitchell, 1977, 2018). It was formed during the subduction of the Neo-Tethys from the Late Cretaceous to the Eocene (Mitchell, 1977, 2018; Beckinsale, 1979; Mitchell and Garson, 1981; Bender, 1983; Gardiner et al., 2015a; Li, J.X., et al., 2018, 2019; Mao et al., 2020).

Over half of the historical and current Sn production in Southeast Asia was mined from placer deposits (Sainsbury, 1969; Lehmann et al., 2020). The fortunate combination of deep tropical weathering and the Pliocene-Quaternary marine transgression in Southeast Asia caused trapping of alluvial sediments in flooded valleys (Chhibber, 1934; Beckinsale, 1979; Schwartz et al., 1995; Mitchell, 2018). Abundant placer Sn deposits were formed in Peninsular Myanmar when primary tin deposits exposed at surface were eroded and materials were carried to the alluvial flats (Penzer, 1922; Clegg, 1944a, b; Bender, 1983).

Tin mineralization in Myanmar

Tin mineralization associated with all three tin belts has been discovered in Myanmar (Figs. 1–3; Htun et al., 2017; Mitchell, 2018). For example, the Wan Pon Sn occurrence in the easternmost corner of Myanmar is related to a granitoid pluton, which likely belongs to the Eastern granite province (Figs. 1, 3; Sone and Metcalfe, 2008; Htun et al., 2017; Cong et al., 2021), although geochronological studies of this mineralization are still unavailable. A surge of tin production in Myanmar since 2013 was mainly due to tin mining from the Man Makhsan tin deposits, Wa State, which elevated Myanmar to be the third largest global tin producer (Gardiner et al., 2015b). Geologic details of the Man Makhsan tin district are currently unavailable, but an adjacent granite pluton was inferred to belong to the north extension of the Central granite province in Thailand, formed in the Late Triassic (Htun et al., 2017; Mitchell, 2018). Numerous Sn deposits distributed in the Slate belt belong to the Western tin belt, which is connected to Sn mineralization in the Tengchong block (Figs. 1, 2, 4; Mitchell, 1977, 2018; Wang et al., 2014).

This study mainly focuses on six primary Sn deposits—from north to south, the Mong Kan Noi (20.62° N, 98.75° E), Padatchaung (19.66° N, 96.61° E), Mawchi (18.82° N, 97.16° E), Hermyingyi (14.25° N, 98.35° E), Bwabin (14.16° N, 98.39° E), and Pagaye (14.09° N, 98.32° E) deposits—and two placer Sn deposits, including Ohnbinkwin (14°37' N, 98°00' E) and Bang-I-Tang (14°40' N, 98°16' E; Figs. 2, 3).

Primary deposits: The Mong Kan Noi deposit is located in the Mong Ton Township, Shan State (Figs. 2, 3). A total of 24 cassiterite- and wolframite-bearing quartz veins were observed in Mong Kan Noi. These veins are mainly hosted in highly weathered granite and are generally northwest trending with widths ranging from 20 cm to 2.5 m and dipping at angles varying from 65° to 85° (S.M.T.L. Paw and S.H. Doh, unpub. report, 2018). All the other primary deposits are located in the Slate belt (Fig. 2). The Padatchaung W (Sn) deposit is located ~40 km to the east of the Pyimana Township, Mandalay Division. The Mawchi mine, situated ~219 km to the southeast of Naypyitaw, is a world-class Sn-W deposit, with estimated ore reserves of 350,000 tonnes (Myint et al., 2018). The Bwabin, Hermyingyi, and Pagaye Sn deposits are located to the northeast of Dawei (Tavoy) City (Fig. 2). Tin and tungsten ores in these primary deposits generally occur near the granite boundary (Clegg, 1944a, b; Zaw, 1990; Gardiner et al., 2014a, b; Jiang et al., 2017; Myint et al., 2017; Mitchell, 2018; Mao et al., 2020). The width of cassiterite- and wolframite-bearing veins varies from centimeters to over 2 m (Fig. 5). All the veins dip steeply, and the lengths of individual veins can be over 200 m. Greisenization occurred in the granite on both sides of the quartz veins with alteration to muscovite

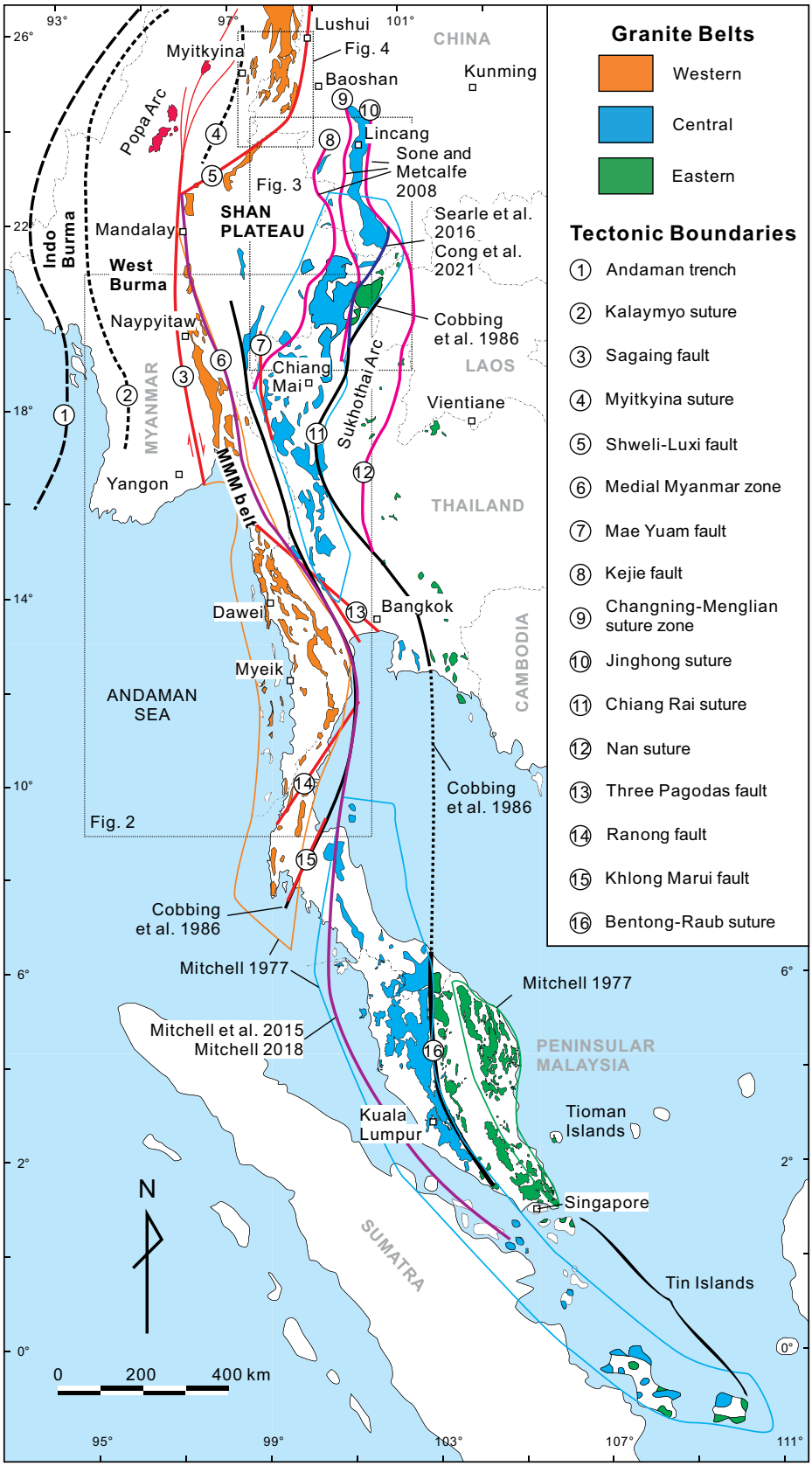

Fig. 1. Simplified map showing the granite belts, tin mineralization belts, and tectonic boundaries in Southeast Asia. Modified after Mitchell (1977, 2018), Cobbing et al. (1986), Sone and Metcalfe (2008), Mitchell et al. (2015), Searle et al. (2016), and Cong et al. (2021).

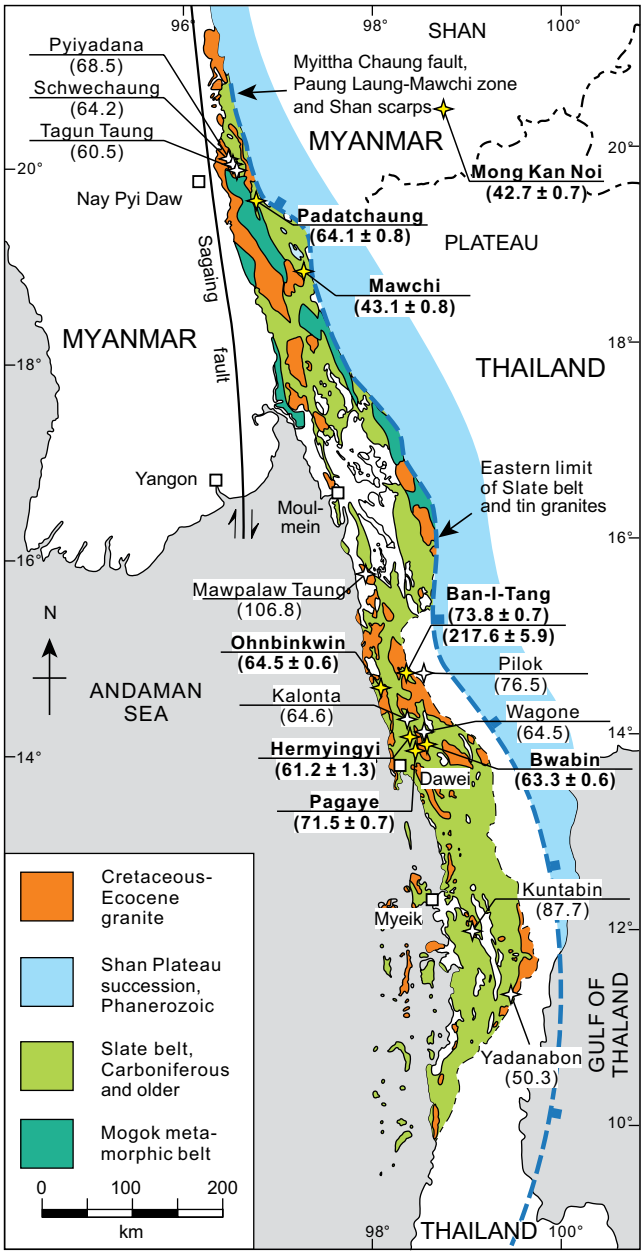

Fig. 2. Geologic map of the Western tin belt in Myanmar with the distribution of selected Sn deposits. Modified after Mitchell et al. (2021).

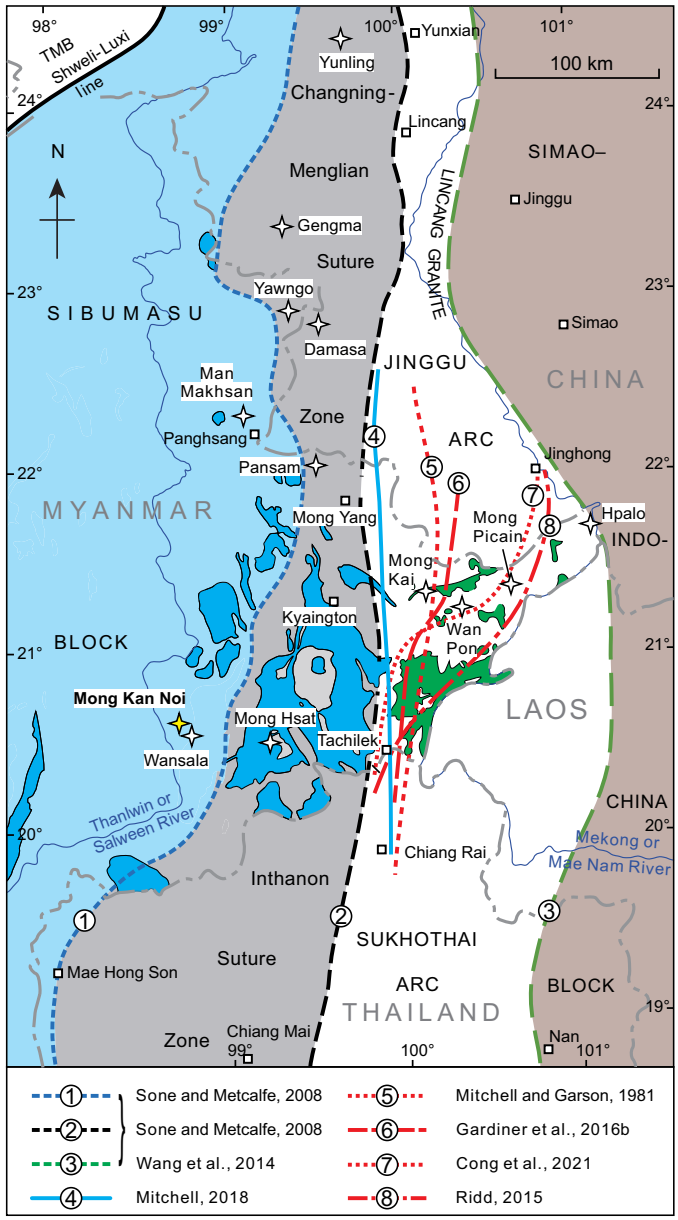

Fig. 3. Geologic map of eastern Myanmar showing the proposed tectonic boundaries and selected Sn deposits. Modified after Mitchell (2018). TMB = Tagaunge Myitkyina belt.

and quartz in all the studied primary deposits (Fig. 5B-D). Ore minerals are dominantly cassiterite and wolframite in the studied primary deposits, with minor molybdenite, pyrite, chalcopyrite, pyrrhotite, sphalerite, galena, arsenopyrite, bismuthinite, and bismuth (Fig. 5G-I).

Placer deposits: The Dawei district hosts over 200 primary and placer tin mines in an area of 13,500 km^2. Areas running along the Heinze Chaung (Heinze River) are very productive for placer tin ores (Figs. 6, 7). Cassiterite was mined from eluvial and alluvial placers up to 30 m thick. Tin content varies significantly, from several kilograms to a few grams per cubic meter, consistent with the heterogeneous nature of these placer deposits. The Ohnbinkwin deposit is located in the valley of the Heinze Chaung close to where the Ohnbinkwin Chaung merges into the main stream (Figs. 6, 7A). The Bang-I-Tang deposit is located in a valley near the Thai-Myanmar border (Figs. 6, 7B).

Methods

Cathodoluminescence

Scanning electron microscopy-cathodoluminescence (SEM-CL) images of zircon and cassiterite were obtained at the Beijing Geoanalysis Co., Ltd with a JEOL JSM6510 scanning electron microscope equipped with a Gatan CL detector. An acceleration voltage of 15 kV, a probe current of ~6 nA, and a magnification of ~250× were used for zircon. An acceleration

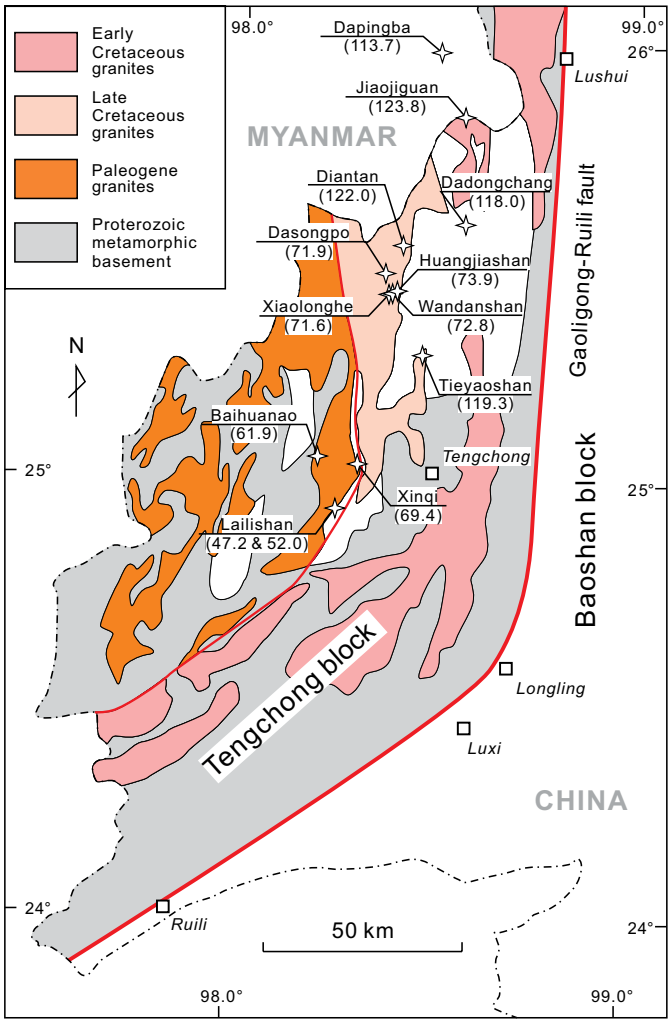

Fig. 4. Geologic map of the Tengchong block and selected Sn deposits. Modified after Chen et al. (2014).

voltage of 15 kV, a probe current of ~6 nA, and a magnification of ~100× to 200× were used for cassiterite.

Laser ablation-inductively coupled plasma-mass spectrometry (LA-ICP-MS) U-Pb dating

Zircon, cassiterite, and wolframite LA-ICP-MS U-Pb dating was conducted at the State Key Laboratory of Ore Deposit Geochemistry, Institute of Geochemistry, Chinese Academy of Sciences, Guiyang. The analytical system is composed of a GeoLas Pro 193-nm ArF excimer laser ablation system and an Agilent 7500× ICP-MS instrument. Helium was used as carrier gas and was mixed with argon via a T connector before entering the ICP-MS. Around six preablation pulses before each analysis were applied to remove surface contamination of cassiterite. Each analysis included 20 s of background reading followed by 36 s of data acquisition. During laser ablation, fluid/mineral inclusions were occasionally ablated, resulting in anomalous spikes of signals. These analyses were terminated and replaced with new spots to ensure that none of the results were contaminated. The time dependent drift of U-Pb ratios was corrected by conventional standard-sample bracketing method.

Zircon U-Pb analysis was carried out with a laser energy density of 5 J/cm^2, a repetition rate of 5 Hz, and a spot size of 32 µm. The zircon standard 91500 was used as external standard for zircon U-Pb dating (Wiedenbeck et al., 1995). The zircon standard Plešovice was analyzed as the unknown and returned a weighted average U-Pb age of 337.1 ± 2.4 Ma (n = 9; mean square of weighted deviates [MSWD] = 0.01), which is identical to the recommended isotope dilution-thermal ionization mass spectrometry (ID-TIMS) age of 337.13 ± 0.37 Ma (Sláma et al., 2008). Cassiterite U-Pb dating was conducted with a laser energy density of 8 J/cm^2, a repetition rate of 7 Hz, and a spot size of 44 µm. An in-house cassiterite standard AY-4 was used as external standard for cassiterite U-Pb dating. AY-4 was collected from the Furong tin deposit in Hunan Province, South China and has an ID-TIMS U-Pb age of 158.2 ± 0.4 Ma (Yuan et al., 2011). AY-4 was analyzed three to four times every eight to 10 analyses of unknown samples. A few of the AY-4 analyses were removed from the standard list during data reduction, as their signals demonstrated the presence of common lead. An in-house cassiterite standard from the Dachang Sn deposit was used for quality control and returned the age of 91.7 ± 2.2 Ma (n = 48; MSWD = 0.47), consistent with the age of 90.4 ± 1.8 Ma from Tang et al. (2020). Mao et al. (2020) reported that the current analytical precision of the U-Pb dating method on cassiterite cannot distinguish different generations of cassiterite in a single cassiterite grain, so in most cases (>80%) we performed one spot analysis on each grain, and in a few cases analyzed an individual cassiterite grain more than once. Wolframite U-Pb dating was conducted with a laser energy density of 5 J/cm^2, a repetition rate of 6 Hz, and a spot size of 60 µm. NIST612 and an in-house wolframite standard MTM were used as external isotopic calibration standards. MTM was well constrained using the ID-TIMS method with a U-Pb age of 334.4 ± 1.7 Ma (Harlaux et al., 2018). Another in-house wolframite standard NM was used for quality control and yielded a lower intercept age of 140.0 ± 1.3 Ma (n = 10; MSWD = 0.13), consistent within error with the age of 142.3 ± 1.3 Ma by Tang et al. (2020).

Off-line selection and integration of background and analyte signals, time-drift correction, and quantitative calibration for U-Pb dating were performed by the ICPMSDataCal program (Liu et al., 2008, 2010) following the method of Yuan et al. (2008) and Tang et al. (2020). Concordia diagrams and weighted mean age calculations were made using the Isoplot program (Ludwig, 2003). Cassiterite and wolframite typically contain some common lead; therefore, the Tera-Wasserburg U-Pb concordia diagram was used to obtain a date from the lower intercept in this plot.

Molybdenite Re-Os dating

Molybdenite Re-Os dating was conducted at the State Key Laboratory of Isotope Geochemistry, Guangzhou Institute of Geochemistry, Chinese Academy of Sciences, Guangzhou. Samples, to which a ^{185}Re spike and common Os standard were added, were loaded and sealed in Carius tubes and digested with aqua regia at 200°C for over 24 h. After cooling of the solution, Os was separated from Re by CCl_4 extraction and purified by microdistillation. Rhenium was separated from the major matrix elements (e.g., Mo, W, and Fe) by solvent extraction with N-benzoyl-N-phenylhydroxylamine

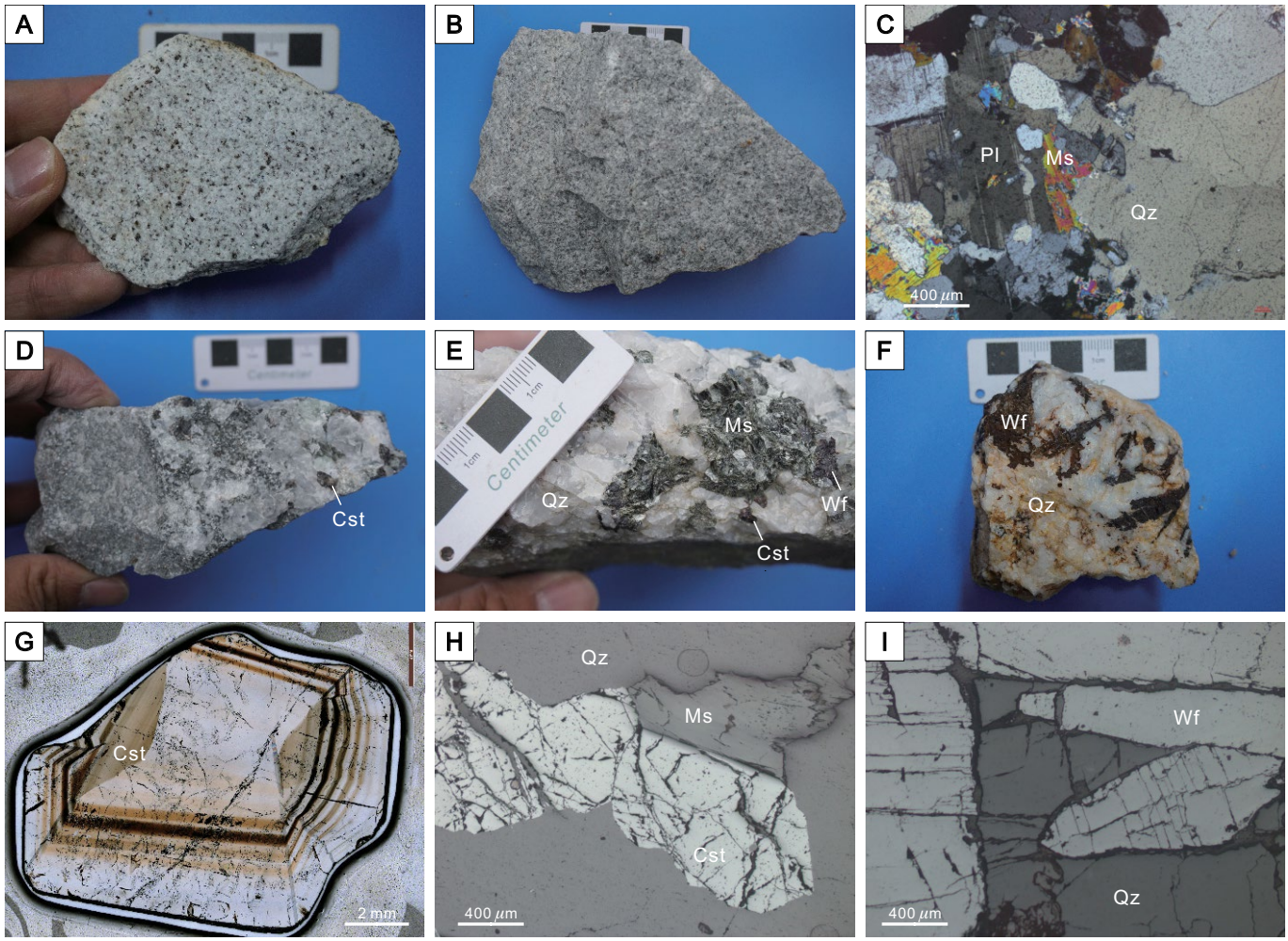

Fig. 5. (A-C) Photos and cross-polarized images of granites. (D-F) Hydrothermal veins with cassiterite-wolframite-sulfide mineralization. (G-I) Transmitted-light and reflected-light images of cassiterite and wolframite. A is from the Mong Kan Noi deposit, B-D from the Hermyingyi deposit, E and H from the Bwabin deposit, F and I from the Padatchaung deposit, and G from the Mawchi deposit. The Mong Kan Noi granite is a medium- to fine-grained two-mica granite, which contains ~30% quartz, ~50% feldspar, ~10% muscovite, and 10% biotite. The Hermyingyi granite is medium- to fine-grained muscovite granite, which contains ~30% quartz, ~55% feldspar, ~14% muscovite, and minor biotite. Abbreviations: Cst = cassiterite, Ms = muscovite, Pl = plagioclase, Qz = quartz, Wf = wolframite.

in chloroform solution (Du et al., 2004; Li et al., 2010). The purified Re and Os were then analyzed by negative-thermal ionization mass spectrometry (N-TIMS) on a Thermo-Finnigan Triton (Creaser et al., 1991). Procedural blanks are in average 4.5 ± 2.3 pg for Re, 0.52 ± 0.02 pg for Os, and 0.29 ± 0.01 for $^{187}Os/^{188}Os$ (n = 3, 2sd). All data were corrected for the procedural blanks. The ^{187}Re decay constant of 1.666 × 10^{-11} $year^{-1}$ (Smoliar et al., 1996) was used to calculate model ages. Molybdenite standard JDC was analyzed and returned the model age of 140.0 ± 0.76 Ma, which is identical to the recommended model age of 139.6 ± 3.8 Ma (Du et al., 2004).

Results

Zircon U-Pb ages of granites

Many zircons of granites from the Hermyingyi deposit and the Mong Kan Noi deposit have irregular grain boundaries and show complex CL textures, indicating that they were modified by successive geologic processes. Therefore, we only analyzed zircon grains with euhedral crystal shapes and clear oscillatory zonation in CL images (Fig. 8). The LA-ICP-MS U-Pb results of zircon analyses are presented in Appendix 1. Zircons from the Hermyingyi deposit have Th contents varying from 218 to 3,677 ppm, with an average of ~942 ppm, and uranium contents ranging from 303 to 14,677 ppm, with an average of ~3,778 ppm. All analytical results cluster tightly on the concordia curve and yield a weighted mean $^{206}Pb/^{238}U$ age of 62.7 ± 0.7 Ma (MSWD = 0.23; n = 10; Fig. 8A). Zircons from Mong Kan Noi have Th contents varying from 34 to 1,137 ppm, with an average of ~531 ppm, and U contents ranging from 442 to 2,952 ppm, with an average of ~1,294 ppm. Analytical results cluster tightly on the concordia curve and yield a weighted mean $^{206}Pb/^{238}U$ age of 216.9 ± 1.8 Ma (MSWD = 0.90; n = 17; Fig. 8B).

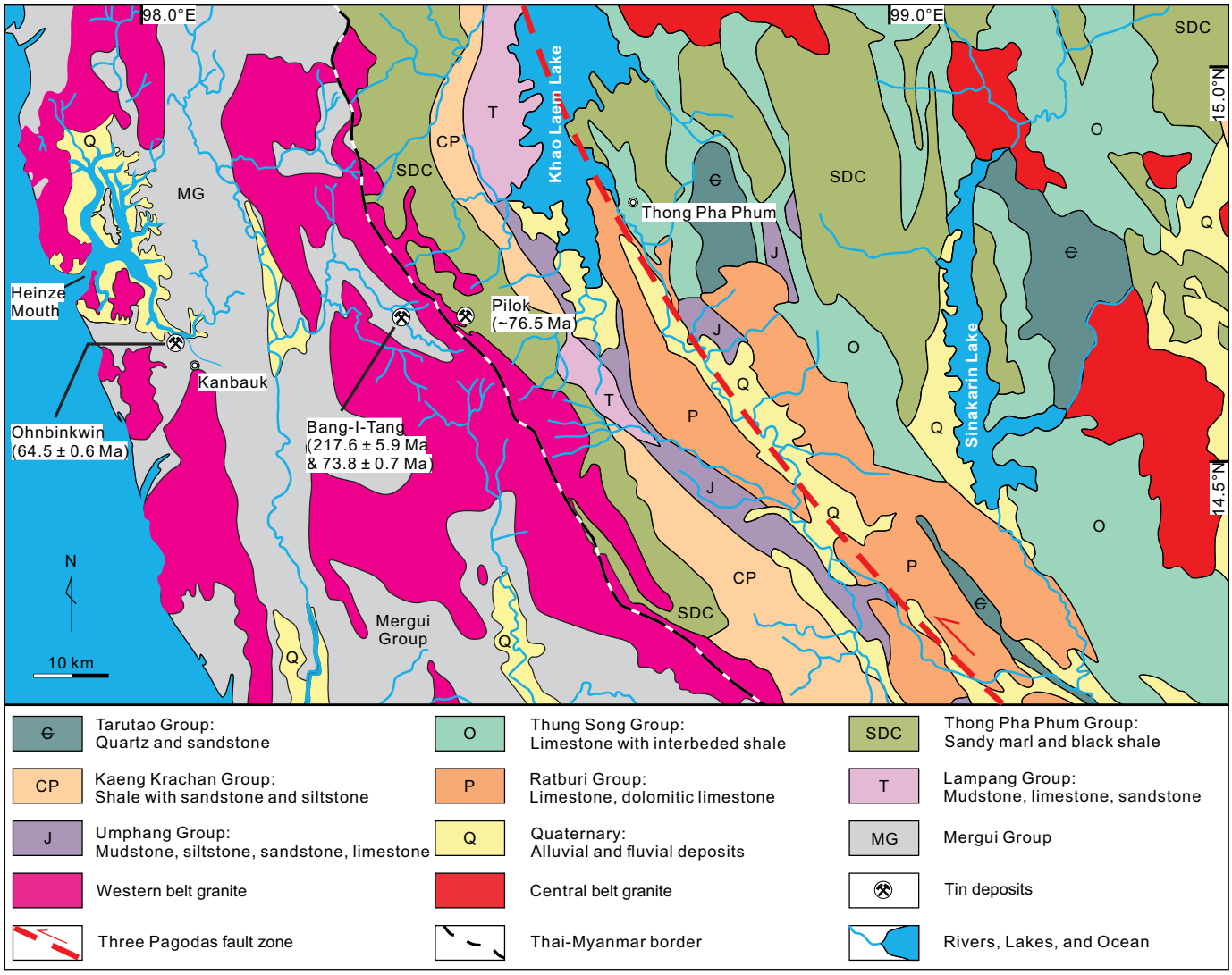

Fig. 6. Geologic map of the Kanbauk-Thong Pha Phun area. Modified after Myanmar Geosciences Society (2014) and Ridd et al. (2011).

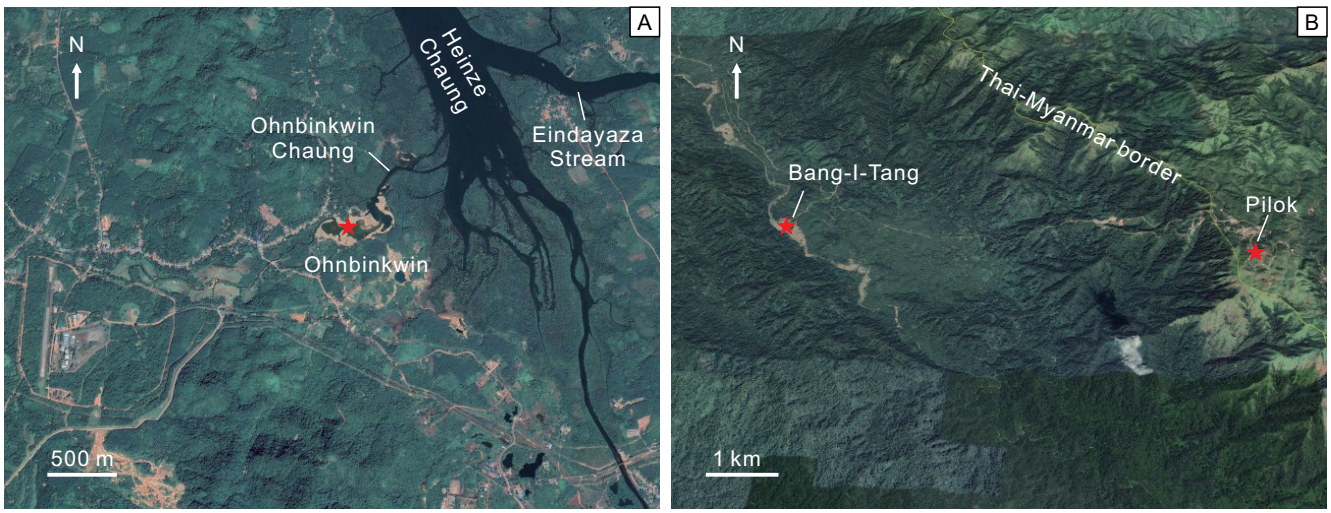

Fig. 7. (A, B) Google maps showing the locations of the Ohnbinkwin and Bang-I-Tang deposits.

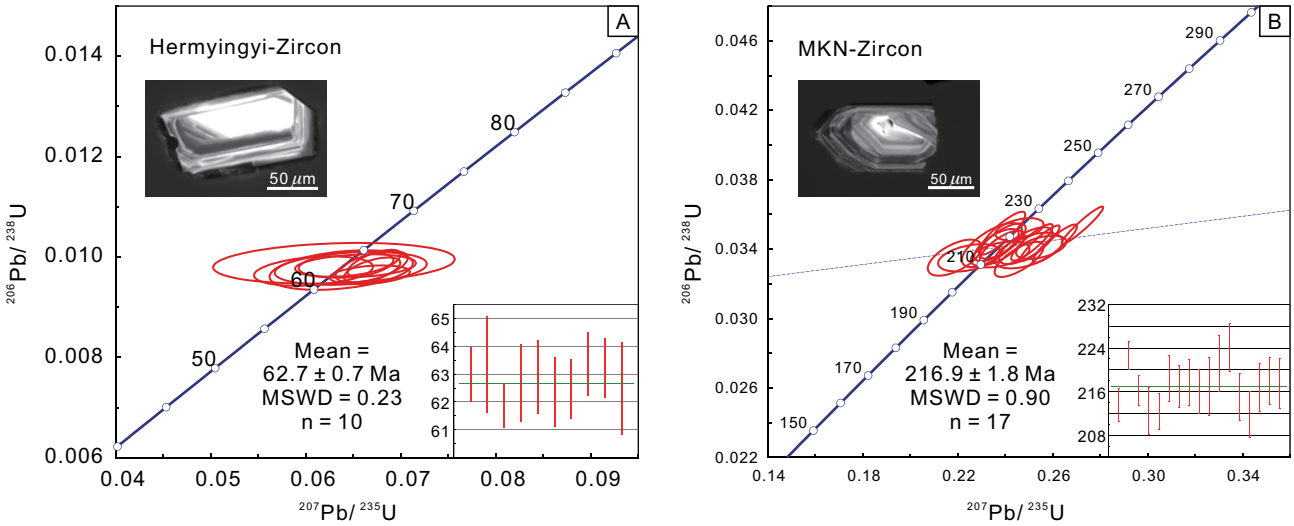

Fig. 8. (A, B) Zircon cathodoluminescence images, U-Pb concordia, and weighted mean age diagrams for granites from the Hermyingyi and Mong Kan Noi (MKN) deposits. MSWD = mean square of weighted deviates.

Cassiterite U-Pb ages of primary deposits

Cassiterite grains from the Pagaye, Bwabin, Hermyingyi, Mawchi, and Mong Kan Noi deposits typically show euhedral crystal shapes with up to 3 mm size in hand samples. Many of the cassiterite grains have dark-gray CL images with very clear and thin oscillatory zones parallel to the growth zones, and the CL intensity varies significantly in different grains (Fig. 9).

Appendix 2 presents the analytical results of U and Pb isotope measurements and related parameters for cassiterite from these deposits. Uranium contents in cassiterite vary from 1.81 to 60.1 ppm (avg ~23.8 ppm) for the Pagaye deposit, from 2.99 to 253 ppm (avg ~75.6 ppm) for the Bwabin deposit, from 2.13 to 20.2 ppm (avg ~8.17 ppm) for the Hermyingyi deposit, from 1.99 to 65.8 ppm (avg ~13.9 ppm) for the Mawchi deposit, and from 1.37 to 59.6 ppm (avg ~13.6 ppm) for the Mong Kan Noi deposit.

The lower intercept ages in the Tera-Wasserburg U-Pb concordia diagrams are as follows: 71.5 ± 0.7 Ma (MSWD = 0.12; n = 30; Fig. 9A) for Pagaye; 63.3 ± 0.6 Ma (MSWD = 0.43; n = 30; Fig. 9C) for Bwabin; 61.2 ± 1.3 Ma (MSWD = 0.10; n = 29; Fig. 9D) for Hermyingyi; 43.1 ± 0.8 Ma (MSWD = 0.10; n = 42; Fig. 9E) for Mawchi; and 42.7 ± 0.7 Ma (MSWD = 0.21; n = 30; Fig. 9F) for Mong Kan Noi.

Cassiterite U-Pb ages of placer deposits

Eighty-five cassiterite grains were analyzed for the Ohnbinkwin deposit (App. 2). Uranium contents vary from 0.70 to 36.2 ppm, with an average of ~9.57 ppm. The majority of the $^{238}U/^{206}Pb$ ratios are >80, and the lowest $^{238}U/^{206}Pb$ ratio is 12.5 (Fig. 10A). Except for some outliers, the majority of these analyses (n = 73, group 1 in App. 2) define a good linear correlation and yield a lower intercept age of 64.5 ± 0.6 Ma (MSWD = 0.63). The spot with the lowest $^{238}U/^{206}Pb$ ratio and highest $^{207}Pb/^{206}Pb$ ratio isolated from the rest of the data is used for the acquisition of the lower intercept, although removal of this spot makes negligible change to the final result (Fig. 10A). Twenty-five of these ages are concordant and yield a weighted mean $^{238}U/^{206}Pb$ age of 65.0 ± 0.9 Ma (MSWD = 0.37). Twelve spots (gray spots in Fig. 10A) deviating from the general trend are not used for the calculation of the lower intercept age, four of which are concordant (OKB-52 at 72.6 ± 3.1 Ma, OBK-65 at 60.8 ± 2.8 Ma, OBK-79 at 68.8 ± 3.2 Ma, OBK-81 at 68.9 ± 2.9 Ma). The histogram for concordant ages from all the analyses shows a notable peak at ~65 Ma (Fig. 10C).

Seventy-five cassiterite grains were analyzed for the Bang-I-Tang deposit (App. 2). Uranium contents vary from 0.24 to 86.8 ppm, with an average of ~12.1 ppm. Except for some outliers, these analyses generally fall into two groups with good linear correlations (Fig. 10B). Twelve analyses from group 1 define a lower intercept age of 217.6 ± 5.9 Ma (MSWD = 0.09). Five of them are concordant ages and yield a weighted mean $^{238}U/^{206}Pb$ age of 217.2 ± 6.9 Ma (MSWD = 0.09). Forty-nine analyses from group 2 define a lower intercept age of 73.8 ± 0.7 Ma (MSWD = 0.17). Twenty of them are concordant and yield a weighted mean $^{238}U/^{206}Pb$ age of 73.7 ± 0.9 Ma (MSWD = 0.19). Fourteen spots (gray spots in Fig. 10B) fall neither in group 1 nor group 2, six of which are concordant ages (BIT-25 at 66.8 ± 1.8 Ma; BIT-28 at 84.1 ± 2.6 Ma; BIT-50 at 60.5 ± 2.3 Ma; BIT-54 at 60.9 ± 4.0 Ma; BIT-57 at 109.1 ± 9.7 Ma; BIT-64 at 78.8 ± 3.3 Ma). The histogram for concordant ages from all the analyses shows two notable peaks at 75–70 Ma and 220–215 Ma (Fig. 10D).

Wolframite U-Pb age

Uranium contents in wolframite vary from 1.93 to 74.8 ppm (avg ~28.2 ppm) for the Padatchaung deposit (App. 3). Twenty-nine analyses yield a lower intercept age of 64.1 ± 0.8 Ma in the Tera-Wasserburg U-Pb concordia diagram (MSWD = 0.77; Fig. 9B).

Molybdenite Re-Os ages

Analytical results of Re-Os isotopes of molybdenite are listed in Appendix 4. Rhenium contents of molybdenite from the Bwabin deposit vary from 179.9 to 1,214 ppb, with an average of ~642.2 ppb. Model ages of molybdenite range from 63.0 to

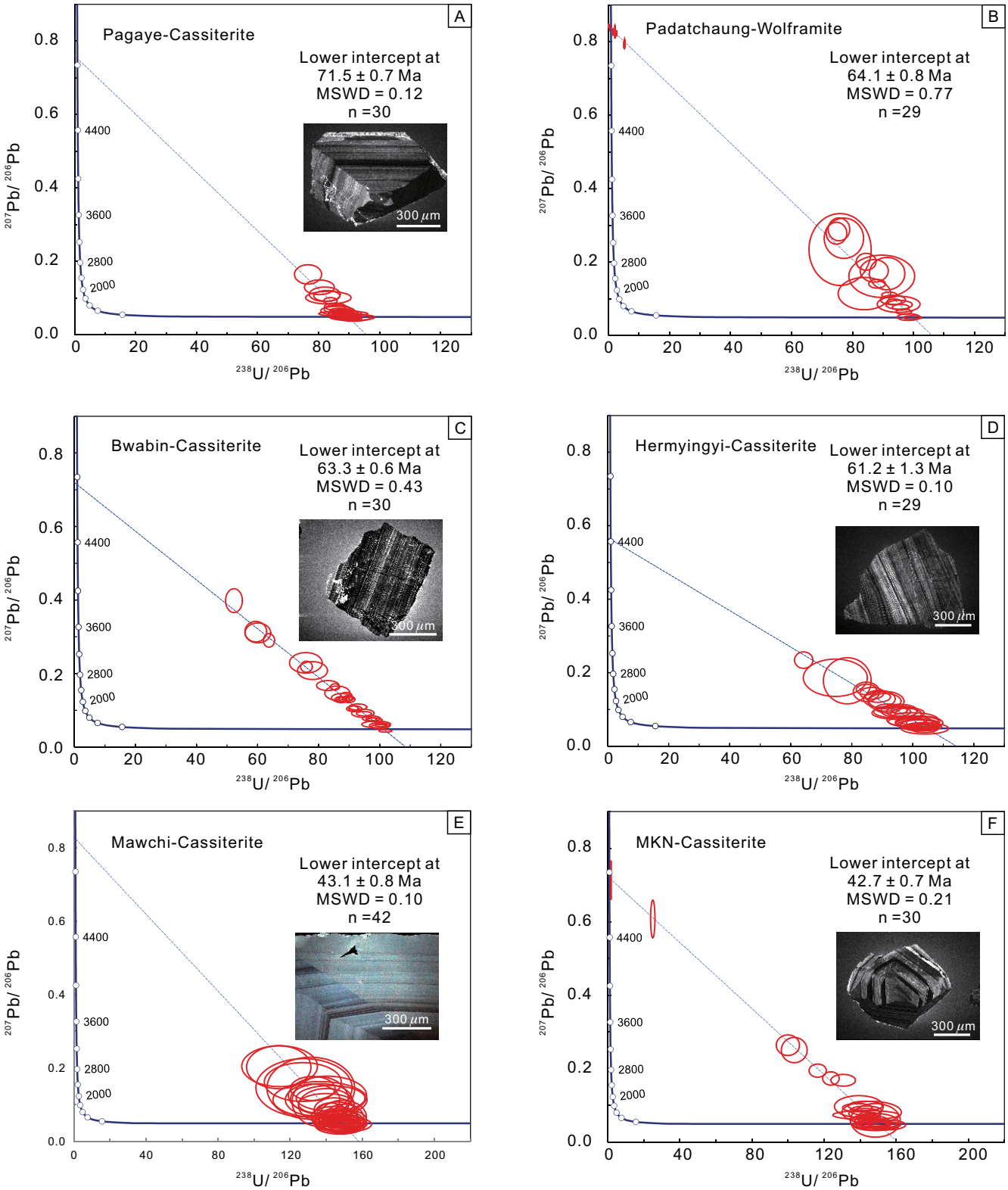

Fig. 9. (A-F) Tera-Wasserburg U-Pb concordia diagrams for cassiterites and wolframites from the Pagaye, Padatchaung, Bwabin, Hermyingyi, Mawchi, and Mong Kan Noi (MKN) deposits. MSWD = mean square of weighted deviates.

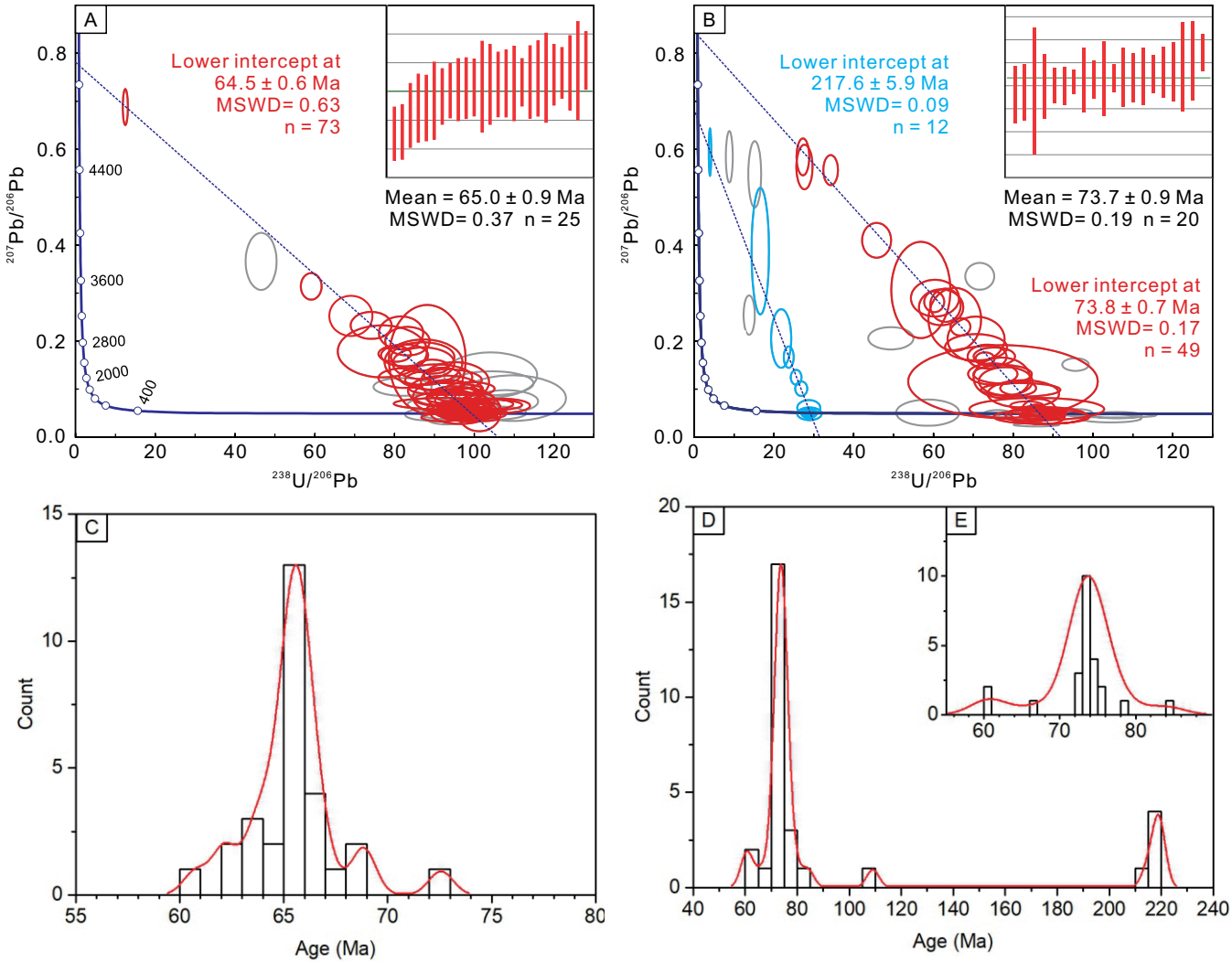

Fig. 10. (A-E) Tera-Wasserburg U-Pb concordia diagrams, weighted mean $^{238}U/^{206}Pb$ ages, and histograms for cassiterites from the Ohnbinkwin and Bang-I-Tang deposits. Histograms were constructed with concordant ages from all the analyses of each deposit. MSWD = mean square of weighted deviates.

57.6 Ma for the Bwabin deposit and from 65.0 to 57.7 Ma for the Hermyingyi deposit.

Discussion

Tin mineralization ages in Myanmar

Htun et al. (2017) reported a zircon U-Pb age of 214 ± 1.5 Ma for the altered biotite granite at the Mong Kan Noi deposit in the Shan Plateau (Figs. 2, 3). Our zircon U-Pb age (216.9 ± 1.8 Ma) of the granite is consistent with their data. However, the cassiterite U-Pb age (42.7 ± 0.7 Ma) shows that Sn mineralization in Mong Kan Noi occurred in the Eocene and that the Triassic granite is the ore-hosting and not the ore-forming granite. Geochronology of zircon, molybdenite, and muscovite indicates that the Mawchi mineralization formed at ~43 to 40 Ma (Myint et al., 2018). Our cassiterite U-Pb age of 43.1 ± 0.8 Ma confirms that the Mawchi deposit was formed in the Eocene. Together with the Yadanabon deposit (~50.3 Ma) in southernmost Myanmar, the Lailishan deposit (~52.0 and 47.2 Ma) in western Yunnan and the Samoeng deposit (~49 Ma) in northwest Thailand, they record the Eocene Sn mineralization event, which is not only distributed in the Western tin belt, but also extends to the Central tin province (Fig. 2; App. 5).

Cassiterite U-Pb dating reveals that the Pagaye deposit was formed in the Late Cretaceous (71.5 ± 0.7 Ma). J.X. Li et al. (2018) reported cassiterite U-Pb ages of 62.5 ± 1.0 and 60.7 ± 3.9 Ma for the Bwabin (Bawapin) deposit, which are consistent within errors with our cassiterite U-Pb age of 63.3 ± 0.6 Ma for Bwabin. Lehmann and Mahawat (1989) reported a Rb-Sr isochron age of 59.5 ± 1.4 Ma for the Hermyingyi stock. H. Li et al. (2018) reported a zircon U-Pb age of 61.4 ± 0.6 Ma for the Hermyingyi granite. Our zircon U-Pb age (62.7 ± 0.7 Ma) and cassiterite U-Pb age (61.2 ± 1.3 Ma) are in good agreement with the above studies for the Hermyingyi deposit. However, Jiang et al. (2017) reported a zircon U-Pb age of 70.0 ± 0.4 Ma for the Hermyingyi monzogranite, and Jiang et al. (2019) reported a Re-Os age of 68.4 ± 2.5 Ma for molybdenite from the Hermyingyi deposit, which suggest that there were multiple episodes of mineralization in the Hermyingyi

deposit. The wide ranges of molybdenite Re-Os model ages in Hermyingyi and Bwabin indicate that these molybdenite samples record a prolonged mineralization in the Paleocene in the Dawei area. Brook and Snelling (1976) obtained an Rb-Sr age of 56 ± 2 Ma and a K-Ar age of 55 ± 1 Ma for the mineralized granite in the Padatchaung deposit. However, the Rb-Sr and K-Ar systems are apt to be disturbed by later thermal events. Our wolframite U-Pb dating shows that W (Sn) mineralization in the Padatchaung deposit occurred at 64.1 ± 0.8 Ma.

Sources of placer Sn deposits

In contrast to zircon, which can be transported by water to over 1,000 km from its origin (Rainbird et al., 1992), placer tin deposits, with cassiterite as the dominant ore mineral, are always found in close proximity to their primary sources (Chhibber, 1934; Mitchell, 2018; Lehmann, 2021). The possibility remains that a placer deposit may have multiple sources, especially if abundant primary deposits cluster in an area like the Dawei district (Fig. 2).

Geochronology of the Ohnbinkwin deposit reveals one dominant source of cassiterite grains with the primary ore-forming age of 64.5 ± 0.6 Ma (Fig. 10A). Geochronology in the Bang-I-Tang deposit shows at least two sources of cassiterite grains. One dominant source (~80%) has the primary ore-forming age of 73.8 ± 0.7 Ma, and the other, less important source (~20%) has the primary age of 217.6 ± 5.9 Ma (Fig. 10B). Both the Ohnbinkwin and Bang-I-Tang deposits are modern alluvial placers; therefore, transportation of materials into these deposits is constrained by the local drainage system. Charusiri et al. (1993) obtained Ar-Ar ages of ~74.4 and ~76.5 Ma for muscovite from wolframite- and cassiterite-bearing veins in the Pilok mine. Although these ages, if not disturbed by later hydrothermal events, are similar to the group 2 age in Bang-I-Tang, the Pilok mine is not likely the major source of the Bang-I-Tang placer deposit, because it is ~10 km to the east and the Thai-Myanmar border serves as the drainage divide to prevent transportation of detrital materials from Pilok to Bang-I-Tang (Figs. 6, 7B). The primary Sn sources are very likely in the Bang-I-Tang valley. Granites in the Slate belt are dominantly Cretaceous to Cenozoic, and the Late Triassic granite nearest to Bang-I-Tang is ~50 km to the northeast, based on previous geologic investigations (Fig. 6). However, recent studies revealed several Late Triassic granites in the Slate belt (Dew et al., 2018; Gardiner et al., 2018; Lin et al., 2019a). Therefore, we infer that there are both Late Triassic and Late Cretaceous magmatism and Sn mineralization in the Bang-I-Tang valley (Fig. 10B).

Aside from the major groups of ages, there are many outliers, and some of them are concordant ages (Fig. 10; App. 2). These concordant ages may indicate other potential primary sources and may have geologic significance. For example, spot BIT-57 (109.1 ± 9.7 Ma) may represent the Early Cretaceous Sn mineralization in Myanmar, which was rarely reported (see discussion below). The other concordant outliers (84.1–60.5 Ma) lie within the Late Cretaceous to Eocene Sn mineralization event in Southern Myanmar (Fig. 2). However, caution should be taken in identifying sources of placer deposits by single spot age, because single spot ages may be affected by large errors. In addition, the ablation of microscale Pb-rich mineral inclusions may also affect the accuracy of single spot ages. Therefore, unless the analytical method can be improved or a larger data set can be obtained, whether the concordant outliers represent contribution from other primary sources remains ambiguous.

Tectonic evolution and Sn mineralization in Myanmar

Our new geochronological data allow us to refine existing models on the tectonic evolution and associated Sn mineralization in Myanmar. Granites in the easternmost corner of Myanmar were formed during subduction of the Paleo-Tethys (Gardiner et al., 2016b; Cong et al., 2021). After closure of the Paleo-Tethys, granites and Sn mineralization were formed in the Shan Plateau east of the Salween River in a collisional setting in the Late Triassic (Mitchell, 1977, 2018; Gardiner et al., 2016b; Cong et al., 2021). For example, the ore-forming granite of the Mong Hsat Sn deposit has a zircon U-Pb age of 214 ± 1.5 Ma (Fig. 3; Htun et al., 2014). Our zircon U-Pb age of ~216.9 ± 1.8 Ma for the granite from the Mong Kan Noi deposit confirms the Late Triassic magmatism in this area. Dew et al. (2018) reported two granite rocks located ~135 km northeast of Myeik, which belongs to the Slate belt in Thailand, with zircon U-Pb ages of ~214 Ma. Gardiner et al. (2018) reported a zircon U-Pb age of 218.9 ± 2.5 Ma for a granite from Payangazu located ~130 km north of Naypyitaw. Together with our cassiterite U-Pb age of 217.6 ± 5.9 Ma from the Bang-I-Tang placer deposit, we confirm a Late Triassic age for magmatism and Sn mineralization in the Western tin belt, which belongs to the west extension of the Central tin belt.

An Early Cretaceous Mondaung arc with a zircon U-Pb age range of 128–113 Ma has been recognized in and east of the Shan scarps between Mandalay and Naypyitaw (Mitchell et al., 2012, 2020a, b, 2021; Lin et al., 2019b). It is connected to the Early Cretaceous granites in the Tengchong block in the north (Fig. 4) and granites in the Mawpalaw Taung area south of Moulmein (Fig. 2). The Early Cretaceous granites were formed during eastward subduction of the Meso-Tethys (Bangong-Nujiang Tethys; Li, J.X., et al., 2018, 2019; Lin et al., 2019a; Mitchell et al., 2021). A series of Early Cretaceous Sn deposits have been reported in the Tengchong block (Fig. 4; App. 5), but the only Early Cretaceous Sn mineralization reported in southern Myanmar is the Mawpalaw Taung tin-bearing pegmatites (106.8 ± 1.6 Ma; Paik, 2017), and no Sn mineralization related to the Mondaung arc has been identified so far (Mitchell et al., 2021).

Most of the granites and related Sn mineralization in the Western tin belt were formed in an Andean-type subduction zone analogous to the Bolivian tin belt (Mitchell and Garson 1981; Mitchell et al., 2012, 2021; Gardiner et al., 2015a; Li, J.X., et al., 2018). Mitchell (1977) inferred a shallow-dipping subduction zone from the Cretaceous to the Eocene along the Andaman trench (Fig. 1). The flat slab reached beneath the Sibumasu terrane at ~90 Ma and generated magmatism and Sn mineralization to form the Kuntabin Sn deposit in southern Myanmar (Mao et al., 2020). Mitchell (1979) suggested that tin granites were generated during crustal thickening and shear heating along the thrust at depth. Alternatively, back-arc extension, induced by slab rollback, was proposed for the generation of the Late Cretaceous to Paleocene tin granites in recent studies (Sanematsu et al., 2014; Jiang et al., 2017; Li et al., 2019).

The initial collision between the Indian and Eurasia continents occurred in Tibet at ~65–63 Ma, then the Neo-Tethys Ocean sutured diachronously both to the west and east (Searle et al., 2007; Royden et al., 2008; Ding et al., 2014). The collision reached western Yunnan before the Eocene, so that the Lailishan deposit was formed in a postcollisional setting (~52.0 and 47.2 Ma; Chen et al., 2014). In contrast, the Neo-Tethys subduction continued in Myanmar through the Late Eocene to form the Shangalon porphyry Cu-Au deposit in the West Burma terrane (~38 Ma; Htut et al., 2020). Although magmatism decreased notably from ~50 to 40 Ma (Fig. 11), Sn mineralization continued in Southeast Asia with continuous subduction of the Neo-Tethys slab to form a series of Eocene Sn deposits (Figs. 2, 4, 11, 12).

The tectonic setting varied significantly since the Permian to form present-day Southeast Asia, and Sn mineralization occurred repeatedly in both collisional and subduction settings to form the world's largest tin province (Figs. 11, 12). The reduced granites crop out in all three belts of the Southeast Asian tin province, indicating that the basement hosted very thick pelitic sedimentary sequences for the generation of reduced melts (Lehmann, 1982, 2021). The reduced tin granites were generated either by melting of the lower crust metasedimentary rocks or by ascent of subduction-related magma through sedimentary rocks and assimilation of carbon (Sanematsu et al., 2014).

Magmatic activity became very weak after ~40 Ma in the Southeast Asian tin province, and Sn mineralization ceased since then (Fig. 11). The India-Eurasia collision has produced eastward and southeastward extrusion of the lithosphere in Southeast Asia (Tapponnier et al., 1990; Royden et al., 2008).

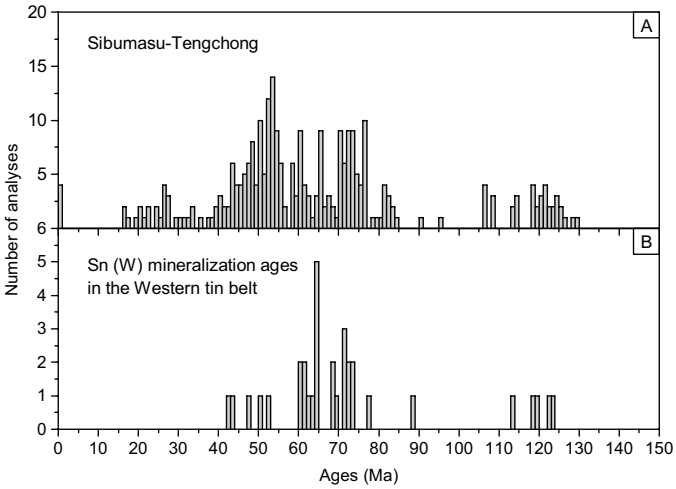

Fig. 11. (A) Igneous rock zircon U-Pb ages from the Sibumasu and Tengchong terranes. (B) Sn (W) mineralization ages in the Western tin belt (App. 5). Magmatism and Sn mineralization in the Sibumasu-Tengchong terrane generally fall into two groups. The Early Cretaceous magmatism and Sn mineralization is comparatively weak. After the gap between 105 and 90 Ma, significant magmatism and mineralization occurred to form abundant Sn deposits in the Western tin belt. Extent of magmatism decreased notably from 50 to 40 Ma, while Sn mineralization continued. Data from Barley et al. (2003), Searle et al. (2007), Mitchell et al. (2012), Dong et al. (2013), Yu et al. (2014), Gardiner et al. (2014a, b, 2015a, 2016a, b, 2017, 2018), Xie et al. (2016), Cao et al. (2017), Crow and Zaw (2017), Jiang et al. (2017), Dew et al. (2018), Li, H., et al. (2018), Li, J.X., et al. (2018), Lin et al. (2019a, b), and references therein.

Lacassin et al. (1997) revealed that the earliest strike-slip fault, the Three Pagodas fault, was activated in the late Eocene (Fig. 1). Xu et al. (2015) proposed that extrusion of the lithosphere and clockwise rotation of the Tengchong block occurred since the late Eocene. Therefore, although the Neo-Tethys subduction continued to generate magmatism and Cu mineralization in the West Burma terrane (Mitchell et al., 2011, 2021), we infer that dextral motion along a series of strike-slip faults and extrusion of the lithosphere after ~40 Ma are responsible for the weakened magmatic activity and terminated Sn mineralization in the Southeast Asian tin province.

Comparison with other world-class tin provinces

Cassiterite U-Pb dating revealed that the earliest Sn mineralization occurred in Archean Sn pegmatite (~2.8 Ga) in Western Australia (Denholm et al., 2021). Proterozoic Sn mineralization has also been reported in South Africa, Brazil, Russia, Rwanda, South China, and Saudi Arabia (Gulson and Jones, 1992; Zhang, R., et al., 2017b; Neymark et al., 2018, 2021; Zhang, S., et al., 2019; Rizvanova and Kuznetsov, 2020); however, pre-Cambrian Sn mineralization is comparatively rare, and the most important Sn provinces all formed during the Phanerozoic (Fig. 12).

Areas of mineralization: Most tin provinces form linear belts along continental margins or major orogenic belts in which granite magma was generated (Sainsbury, 1969). The Cornwall tin province is 200 km in length (Moscati and Neymark, 2020). The Central Andean tin belt stretches for about 900 km (Gemmrich et al., 2021). The South China tin province consists of the 400-km-long Nanling belt, the 250-km-long Southeast Coastal belt, and the 900-km-long belt extending from eastern Yunnan through Guangxi to western Guangdong Province (Yun-Guang belt; Mao et al., 2013). The Southeast Asian tin province hosts the 500-km-long Eastern belt, the over

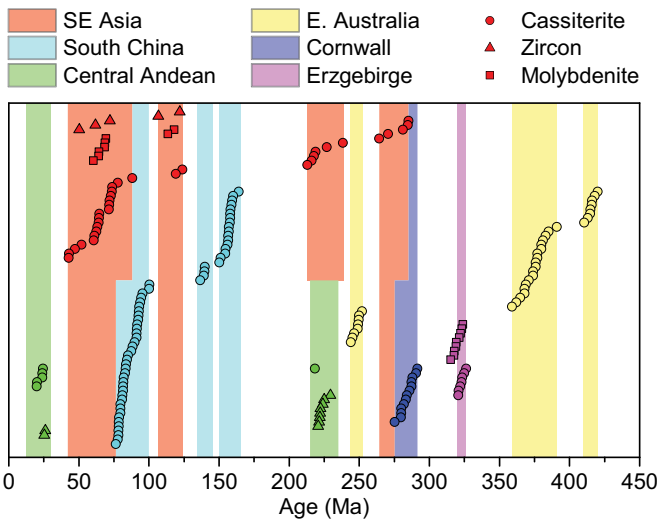

Fig. 12. Compiled cassiterite U-Pb ages (with minor zircon U-Pb and molybdenite Re-Os ages) for Sn mineralization in global tin provinces. Data are from Yuan et al. (2008, 2011), Chen et al. (2014), Li et al. (2016), Qiu et al. (2017), Zhang, R., et al. (2017b), Carr (2018), Li, J.X., et al. (2018), Neymark et al. (2018, 2021), Zhang, S., et al., (2019), Cao et al. (2020), Du et al. (2020), Mao et al. (2020), Moscati and Neymark (2020), Yang, J.H., et al. (2020), Denholm et al. (2021), Gemmrich et al. (2021), Hu et al. (2021), and references therein.

3,000-km-long Central belt, and the 2,000-km-long Western belt, including western Yunnan (Fig. 1; Mitchell, 1977, 2018). The length of mineralization belts is generally proportional to the historical tin production in these tin provinces.

Duration of mineralization events: A particular tectonic setting (e.g., subduction) and related magmatism may prevail for over 100 m.y., but mineralization events typically occur in much shorter periods (Bissig et al., 2008; Sillitoe, 2012). Cassiterite U-Pb geochronology studies have generally revealed shorter durations for Sn mineralization events than previously reported by conventional methods. For example, granite magmatism and related Sn mineralization in the Erzgebirge tin province were grouped into two periods (330–320 and 310–290 Ma) in previous studies. However, systematic U-Pb dating of cassiterite from the Erzgebirge tin province revealed a short mineralization period of ~6 m.y. (326–320 Ma; Fig. 12; Zhang et al., 2017a). Geochronology of granites by conventional methods in the Cornwall tin province constrained magmatic activity to 295–270 Ma, but cassiterite U-Pb dating slightly narrowed the duration of mineralization to ~17 m.y. (292–275 Ma; Moscati and Neymark, 2020). Figure 12 reveals that durations of regional Sn mineralization events are typically in the range of ~5–30 m.y. Our new data suggest a similar to even longer duration of up to ~50 m.y. for Sn mineralization in Southeast Asia associated with Neo-Tethys subduction. (Figs. 11, 12).

Recurrent Sn mineralization: Recurrent Sn mineralization had long been noticed (Schuiling, 1967) and revealed in many tin provinces by conventional methods (e.g., Taylor, 1979; Lehmann, 1990; Schwartz et al., 1995; Breiter et al., 1999; Searle et al., 2012). Cassiterite U-Pb dating has allowed a better temporal resolution of diachronous Sn mineralization (Fig. 12). The Erzgebirge and Cornwall tin provinces both belong to the Acadian-Variscan-Appalachian orogen but were formed in distinct time intervals (Romer and Kroner, 2016). The Eastern Australia tin province, which hosts ~9% of the global tin reserves (USGS, 2020), extends for over 2,000 km and varies in age from Silurian to Triassic (Solomon and Groves, 1994). Cassiterite U-Pb dating revealed three Sn mineralization episodes: ~420–413 Ma in the Lachlan orogen (Carr, 2018), ~391–359 Ma in the Tasmania Islands (Denholm et al., 2021), and ~252–244 Ma in the Mole granite system (Carr, 2018). The South China tin province mainly contains three mineralization belts distinct in space and time: the Nanling belt (~165–150 Ma; Mao et al., 2007, 2013; Yuan et al., 2008, 2011), the Southeast Coastal belt (145–135 Ma; Qiu et al., 2017; Liu et al., 2018), and the Yun-Guang belt (~100–75 Ma; Cheng et al., 2016; Hu et al., 2021). Cassiterite U-Pb dating revealed that Sn mineralization in the Southeast Asian tin province occurred repeatedly in four periods: Permian (~285–265 Ma), Triassic (~239–213 Ma), Early Cretaceous (~124–107 Ma), and Late Cretaceous to Eocene (~90–42 Ma; Figs. 11, 12).

Superimposition of Sn mineralization: Superimposition of Sn mineralization is also well documented in many tin provinces. For example, the Late Cretaceous Sn mineralization in the Guangxi Province is superimposed on the Neo-Proterozoic and Late Triassic Sn mineralization in South China (Feng et al., 2013; Zhang et al., 2019). The Central Andean tin province is genetically related to two major periods of magmatism (Fig. 12). The late Oligocene (~20–13 Ma) mineralization is superimposed on the Late Triassic (~240–220 Ma) mineralization in the northern part of the Central Andean tin province (Lehmann et al., 1990; Gemmrich et al., 2021; Lehmann, 2021). In Southeast Asia, the Eastern tin belt hosts the Late Triassic magmatism and Sn mineralization in eastern Malaysia (Ng et al., 2015; Searle et al., 2016; Liu et al., 2020; Yang, J.H., et al., 2020). The Bulangshan and Mengsong Sn occurrences, located east of the Changning-Mengliang suture in western Yunnan, are related to the Late Triassic granites (Wang et al., 2015). The Central tin belt in eastern Myanmar hosts the Eocene Mong Kan Noi deposit (Figs. 2, 3). The Western tin belt contains the Late Triassic and Early Cretaceous Sn mineralization (Figs. 2, 4), although the economic significance of these earlier mineralization events is negligible compared to the Late Cretaceous to Eocene Sn mineralization.

The fortunate combination of the length of tin mineralization episodes between the Permian and Eocene, the largest surface extension of mineralization, the deep tropical weathering, and the Pliocene-Quaternary marine transgression in Southeast Asia were probably all factors contributing to the formation of the world's largest tin province.

Conclusions

1. Combination of our geochronology work with previous studies has revealed three episodes of Sn mineralization in the Western tin belt of Southeast Asia, including the Late Triassic (~218 Ma), the Early Cretaceous (~124–107 Ma), and the Late Cretaceous to Eocene (~90–42 Ma). The majority of the Sn deposits in this belt were formed during the last mineralization event.
2. Global data compilation reveals that durations of regional Sn mineralization events are typically in the range of ~5–30 m.y. and that the Neo-Tethys subduction in Southeast Asia generated a prolonged Sn mineralization event up to ~50 m.y.
3. The tectonic setting varied significantly in Southeast Asia during the closure of multiple Tethys oceans and back-arc basins, while Sn mineralization occurred recurrently in both subduction and collisional settings. The tectonic setting changed from Neo-Tethys subduction to dextral motion along a series of strike-slip faults in the late Eocene and terminated Sn mineralization in Southeast Asia.
4. The overall length of tin mineralization episodes in Southeast Asia from the Permian to Eocene exceeds that of any other tin province globally and was one of the most important factors in the formation of the exceptional Sn endowments of the Southeast Asian tin province.

Acknowledgments

We thank Dr. Shengling Sun, Yezhi He, and Junjie Han for their assistance during the lab work. This work was financially supported by the National Natural Science Foundation of China (grants 42121003, 42073045, 42073046), K.C. Wong Education Foundation (grant GJTD-2020-13), a special fund managed by the State Key Laboratory of Ore Deposit Geochemistry, and a comprehensive scientific survey for establishing the Gaoligongshan National Park in Yunnan Province (E1UN004000). The manuscript was significantly improved

with the constructive comments from Dr. Andrew Mitchell and Associate Editor Massimo Chiaradia.

REFERENCES

Barley, M.E., Pickard, A.L., Zaw, K., Rak, P., and Doyle, M.G., 2003, Jurassic to Miocene magmatism and metamorphism in the Mogok metamorphic belt and the India-Eurasia collision in Myanmar: Tectonics, v. 22, doi: 10.1029/2002TC001398.

Beckinsale, R.D., 1979, Granite magmatism in the tin belt of South-East Asia, *in* Atherton, M.P., and Tarney, J., eds., Origin of granite batholiths: Boston, Birkhäuser, p. 34–44.

Bender, F., 1983, Geology of Burma: Berlin, Borntraeger, 293 p.

Bissig, T., Ullrich, T.D., Tosdal, R.M., Friedman, R., and Ebert, S., 2008, The time-space distribution of Eocene to Miocene magmatism in the central Peruvian polymetallic province and its metallogenetic implications: Journal of South American Earth Sciences, v. 26, p. 16–35.

Breiter, K., Förster, H.J., and Seltmann, R., 1999, Variscan silicic magmatism and related tin-tungsten mineralization in the Erzgebirge-Slavkovský les metallogenic province: Mineralium Deposita, v. 34, p. 505–521.

Brook, M., and Snelling, N.J., 1976, K/Ar and Rb/Sr age determinations on rocks and minerals from Burma: London, Institute of Geological Science Isotope Geology Unit, Report 76/12.

Cao, H.W., Zhang, S.T., Lin, J.Z., Zheng, L., Wu, J.D., and Li, D., 2014, Geology, geochemistry and geochronology of the Jiaojiguanliangzi Fe-polymetallic deposit, Tengchong County, Western Yunnan (China): Regional tectonic implications: Journal of Asian Earth Sciences, v. 81, p. 142–152.

Cao, H.W., Pei, Q.M., Zhang, S.T., Zhang, L.K., Tang, L., Lin, J.Z., and Zheng, L., 2017, Geology, geochemistry and genesis of the Eocene Lailishan Sn deposit in the Sanjiang region, SW China: Journal of Asian Earth Sciences, v. 137, p. 220–240.

Cao, J., Yang, X., Du, G., and Li, H., 2020, Genesis and tectonic setting of the Malaysian Waterfall granites and tin deposit: Constraints from LA-ICP (MC)-MS zircon U-Pb and cassiterite dating and Sr-Nd-Hf isotopes: Ore Geology Reviews, v. 118, doi: 10.1016/j.oregeorev.2020.103336.

Carr, P.A., 2018, Tourmaline geochemistry and cassiterite geochronology of highly evolved tin granites and their hydrothermal systems in eastern Australia: Ph.D. thesis, Canberra, Australian National University, 248 p.

Charusiri, P., 1989, Lithophile metallogenetic epochs of Thailand: A geological and geochronological investigation: Ph.D. thesis, Kingston, Canada, Queen's University, 809 p.

Charusiri, P., Clark, A.H., Farrar, E., Archibald, D., and Charusiri, B., 1993, Granite belts in Thailand: Evidence from the $^{40}Ar/^{39}Ar$ geochronological and geological syntheses: Journal of Southeast Asian Earth Sciences, v. 8, p. 127–136.

Chen, X.C., Hu, R.Z., Bi, X.W., Li, H.M., Lan, J.B., Zhao, C.H., and Zhu, J.J., 2014, Cassiterite LA-MC-ICP-MS U/Pb and muscovite $^{40}Ar/^{39}Ar$ dating of tin deposits in the Tengchong-Lianghe tin district, NW Yunnan, China: Mineralium Deposita, v. 49, p. 843–860.

Cheng, Y., Mao, J., and Liu, P., 2016, Geodynamic setting of Late Cretaceous Sn-W mineralization in southeastern Yunnan and northeastern Vietnam: Solid Earth Sciences, v. 1, p. 79–88.

Chhibber, H.L., 1934, The mineral resources of Burma: London, Macmillan, 320 p.

Clegg, E.L.G., 1944a, Notes on tin and wolfram with a description of the tin and wolfram deposits of India and Burma: Records of the Geological Survey of India, Bulletin 15, v. 76, p. 1–129.

——1944b, The mineral deposit of Burma: Bombay, Times of India Press, 38 p.

Cobbing, E.J., Mallic, D.I.J., Pitfield, P.E.J., and Teoh, L.H., 1986, The granites of the Southeast Asian tin belt: Journal of the Geological Society, London, v. 143, p. 537–550.

Cobbing, E.J., Pitfield, P.E.J., Darbyshire, D.P.F., and Mallick, D.I.J., 1992, The granites of the South-East Asian tin belt: British Geological Survey, Overseas Memoir 10, p. 1–230.

Cong, F., Wu, F.Y., Li, W.C., Wang, J.G., Hu, F.Y., He, D.F., Ji, W.Q., Lin, W., and Sein, K., 2021, Petrogenesis of the Main Range and Eastern Province granites in eastern Myanmar: New insights from zircon U-Pb ages and Sr-Nd isotopes: Lithos, v. 382–383, doi: 10.1016/j.lithos.2020.105895.

Creaser, R.A., Papanastassiou, D.A., and Wasserburg, G.J., 1991, Negative thermal ion mass-spectrometry of osmium, rhenium, and iridium: Geochimica et Cosmochimica Acta, v. 55, p. 397–401.

Crow, M.J., and Zaw, K., 2017, Geochronology in Myanmar (1964–2017): Geological Society, London, Memoirs, v. 48, p. 713–759.

Davis, D.W., and Krogh, T.E., 2000, Preferential dissolution of ^{234}U and radiogenic Pb from α-recoil-damaged lattice sites in zircon: Implications for thermal histories and Pb isotopic fractionation in the near surface environment: Chemical Geology, v. 172, p. 41–58.

Denholm, J.L., Stepanov, A.S., Meffre, S., Bottrill, R.S., and Thompson, J.M., 2021, The geochronology of Tasmanian tin deposits using LA-ICP-MS U-Pb cassiterite dating: Economic Geology, doi: 10.5382/econgeo.4837.

Dew, R.E.C., Collins, A.S., Glorie, S., Morley, C.K., Blades, M.L., Nachtergaele, S., King, R., Foden, J., De Grave, J., Kanjanapayont, P., Evans, N.J., Alessio, B.L., and Charusiri, P., 2018, Probing into Thailand's basement: New insights from U-Pb geochronology, Sr, Sm-Nd, Pb and Lu-Hf isotopic systems from granitoids: Lithos, v. 320–321, p. 332–354.

Ding, L., Xu, Q., Yue, Y., Wang, H., Cai, F., and Li, S., 2014, The Andean-type Gangdese Mountains: Paleoelevation record from the Paleocene-Eocene Linzhou basin: Earth and Planetary Science Letters, v. 392, p. 250–264.

Dong, F.L., Hou, Z.Q., Gao, Y.F., Zeng, P.S., Jiang, C.X., and Du, A.D., 2005, Re-Os isotopic dating of molybdenite from Dadongchang copper-lead-zinc deposit in Tengchong area, western Yunnan: Mineral Deposits, v. 24, p. 663–668 (in Chinese with English abs.).

Dong, M.L., Dong, G.C., Mo, X.X., Zhu, D.C., Nie, F., Yu, J.C., Wang, P., and Luo, W., 2013, The Mesozoic-Cenozoic magmatism in Baoshan block, western Yunnan and its tectonic significance: Acta Petrologica Sinica, v. 29, no. 11, p. 3901–3913 (in Chinese with English abs.).

Du, A.D., Wu, S.Q., Sun, D.Z., Wang, S.X., Qu, W.J., Markey, R., Stain, H., Morgan, J., and Malinovskiy, D., 2004, Preparation and certification of Re-Os dating reference materials: Molybdenites HLP and JDC: Geostandards and Geoanalytical Research, v. 28, p. 41–52.

Du, G., Yang, X., Cao, J., and Aziz, J.H.A., 2020, Genesis and timing of the Sungai Lembing tin deposit in Pahang, East Malaysia: Constraints from LA-ICP-MS zircon and cassiterite U-Pb dating, geochemical compositions and Sr-Nd-Hf isotopes: Ore Geology Reviews, v. 119, doi: 10.1016/j.oregeorev.2020.103364.

Feng, Z., Kang, Z., Yang, F., Liao, J., and Wang, C., 2013, Geochronology of the Limu W-Sn-Nb-Ta–bearing granite pluton in South China: Resource Geology, v. 63, p. 320–329.

Ganguly, J., and Tirone, M., 2009, Closure temperature, cooling age and high temperature thermochronology, *in* Gupta, A.K., and Dasgupta, S., eds., Physics and chemistry of the Earth's interior: Crust, mantle and core: New York, Springer, p. 89–98.

Gardiner, N.J., Robb, L.J., and Searle, M.P., 2014a, The metallogenic provinces of Myanmar: Applied Earth Science, v. 123, p. 25–38.

Gardiner, N.J., Robb, L.J., and Searle, M.P., 2014b, Myanmar (Burma): Tectonics and metallogeny: Applied Earth Science, v. 122, p. 136–189.

Gardiner, N.J., Searle, M.P., Robb, L.J., and Morley, C.K., 2015a, Neo-Tethyan magmatism and metallogeny in Myanmar—an Andean analogue?: Journal of Asian Earth Sciences, v. 106, p. 197–215.

Gardiner, N.J., Sykes, J.P., Trench, A., and Robb, L.J., 2015b, Tin mining in Myanmar: Production and potential: Resources Policy, v. 46, p. 219–233.

Gardiner, N.J., Robb, L.J., Morley, C.K., Searle, M.P., Cawood, P.A., Whitehouse, M.J., Kirkland, C.L., Roberts, N.M.W., and Myint, T.A., 2016a, The tectonic and metallogenic framework of Myanmar: A Tethyan mineral system: Ore Geology Reviews, v. 79, p. 26–45.

Gardiner, N.J., Searle, M.P., Morley, C.K., Whitehouse, M.P., Spencer, C.J., and Robb, L.J., 2016b, The closure of Palaeo-Tethys in eastern Myanmar and northern Thailand: New insights from zircon U-Pb and Hf isotope data: Gondwana Research, v. 39, p. 401–422.

Gardiner, N.J., Hawkesworth, C.J., Robb, L.J., Whitehouse, M.J., Roberts, N.M.W., Kirkland, C.L., and Evans, N.J., 2017, Contrasting granite metallogeny through the zircon record: A case study from Myanmar: Scientific Reports, v. 7, p. 748–754.

Gardiner, N.J., Searle, M.P., Morley, C.K., Robb, L.J., Whitehouse, M.J., Roberts, N.M.W., Kirkland, C.L., and Spencer, C.J., 2018, The crustal architecture of Myanmar imaged through zircon U-Pb, Lu-Hf and O isotopes: Tectonic and metallogenic implications: Gondwana Research, v. 62, p. 27–60.

Garson, M.S., and Mitchell, A.H.G., 1970, Transform faulting in the Thai Peninsula: Nature, v. 228, p. 45–47.

Gemmrich, L., Torró, L., Melgarejo, J.C., Laurent, O., Vallance, J., Chelle-Michou, C., and Sempere, T.P.A., 2021, Trace element composition and U-Pb ages of cassiterite from the Bolivian tin belt: Mineralium Deposita, doi: 10.1007/s00126-020-01030-3.

Gulson, B.L., and Jones, M.T., 1992, Cassiterite—potential for direct dating of mineral-deposits and a precise age for the Bushveld Complex granites: Geology, v. 20, p. 355–358.
Harlaux, M., Romer, R.L., Mercadier, J., Morlot, C., Marignac, C., and Cuney, M., 2018, 40 Ma of hydrothermal W mineralization during the Variscan orogenic evolution of the French Massif Central revealed by U-Pb dating of wolframite: Mineralium Deposita, v. 53, p. 21–51.
Htun, T., Khositanont, S., and Manaka, T., 2014, Preliminary investigation of new tin deposits in Mong Ton-Mong Hsat area, Shan State (east), Myanmar: Regional Congress on Geology, Mineral and Energy Resources of Southeast Asia, 13th, Sedona Hotel, Yangon, Myanmar, 2014, Conference paper.
Htun, T., Htay, T., and Zaw, K., 2017, Tin-tungsten deposits of Myanmar: Geological Society, London, Memoirs, v. 48, p. 625–647.
Htut, T.Y., Qin, K., Li, G., Sein, K., and Evans, N.J., 2020, Eocene arc magmatism and related Cu-Au (Mo) mineralization in the Shangalon-Kyungalon district, Wuntho-Popa arc, northern Myanmar: Ore Geology Reviews, v. 125, doi: 10.1016/j.oregeorev.2020.103678.
Hu, P.C., Zhu, W.G., Zhong, H., Zhang, R.Q., Zhao, X.Y., and Mao, W., 2021, Late Cretaceous granitic magmatism and Sn mineralization in the giant Yinyan porphyry tin deposit, South China: Constraints from zircon and cassiterite U-Pb and molybdenite Re-Os geochronology: Mineralium Deposita, v. 56, p. 743–765.
Hutchison, C.S., and Taylor, D., 1978, Metallogenesis in SE Asia: Journal of Geological Society, London, v. 135, p. 407–428.
Jiang, H., Li, W.Q., Jiang, S.Y., Wang, H., and Wei, X.P., 2017, Geochronological, geochemical and Sr-Nd-Hf isotopic constraints on the petrogenesis of Late Cretaceous A-type granites from the Sibumasu block, southern Myanmar, SE Asia: Lithos, v. 268, p. 32–47.
Jiang, H., Jiang, S.Y., Li, W.Q., and Zhao, K.D., 2019, Timing and source of the Hermyingyi W-Sn deposit in southern Myanmar, SE Asia: Evidence from molybdenite Re-Os age and sulfur isotopic composition: Journal of Earth Science, v. 30, p. 70–79.
Lacassin, R., Maluski, H., Leloup, P.H., Tapponnier, P., Hinthong, C., Siribhakdi, K., Chuaviroj, S., and Charoenravat, A., 1997, Tertiary diachronic extrusion and deformation of western Indochina: Structural and $^{40}Ar/^{39}Ar$ evidence from NW Thailand: Journal of Geophysical Research: Solid Earth, v. 102, p. 10,013–10,037.
Lehmann, B., 1982, Metallogeny of tin: Magmatic differentiation versus geochemical heritage: Economic Geology, v. 77, p. 50–59.
——1990, Metallogeny of tin: Berlin Heidelberg, Springer, p. 1–211.
——2021, Formation of tin ore deposits: A reassessment: Lithos, v. 402–403, article 105756.
Lehmann, B., and Mahawat, C., 1989, Metallogeny of tin in central Thailand: A genetic concept: Geology, v. 17, p. 426–429.
Lehmann, B., Ishihara, S., Michel, H., Miller, J., Rapela, C.W., Sanchez, A., Tistl, M., and Winkelmann, L., 1990, The Bolivian tin province and regional tin distribution in the Central Andes: A reassessment: Economic Geology, v. 85, p. 1044–1058.
Lehmann, B., Zoheir, B.A., Neymark, L.A., Zeh, A., Emam, A., Radwan, A.M., Zhang, R., and Moscati, R.J., 2020, Monazite and cassiterite U-Pb dating of the Abu Dabbab rare-metal granite, Egypt: Late Cryogenian metalliferous granite magmatism in the Arabian-Nubian Shield: Gondwana Research, v. 84, p. 71–80.
Li, C.Y., Zhang, R.Q., Ding, X., Ling, M.X., Fan, W.M., and Sun, W.D., 2016, Dating cassiterite using laser ablation ICP-MS: Ore Geology Reviews, v. 72, p. 313–322.
Li, H., Myint, A.Z., Yonezu, K., Watanabe, K., Algeo, T.J., and Wu, J.H., 2018, Geochemistry and U-Pb geochronology of the Wagone and Hermyingyi A-type granites, southern Myanmar: Implications for tectonic setting, magma evolution and Sn-W mineralization: Ore Geology Reviews, v. 95, p. 575–592.
Li, J., Zhong, L.F., Tu, X.L., Liang, X.R., and Xu, J.F., 2010, Determination of rhenium content in molybdenite by ICP-MS after separation of the major matrix by solvent extraction with N-benzoyl-N-phenylhydroxalamine: Talanta, v. 81, p. 954–958.
Li, J.X., Zhang, L.Y., Fan, W.M., Ding, L., Sun, Y.L., Peng, T.P., Li, G.M., and Sein, K., 2018, Mesozoic-Cenozoic tectonic evolution and metallogeny in Myanmar: Evidence from zircon/cassiterite U-Pb and molybdenite Re-Os geochronology: Ore Geology Reviews, v. 102, p. 829–845.
Li, J.X., Fan, W.M., Zhang, L.Y., Evans, N.J., Sun, Y.L., Ding, L., Guan, Q.Y., Peng, T.P., Cai, F.L., and Sein, K., 2019, Geochronology, geochemistry and Sr-Nd-Hf isotopic compositions of Late Cretaceous-Eocene granites in southern Myanmar: Petrogenetic, tectonic and metallogenic implications: Ore Geology Reviews, v. 112, doi: 10.1016/j.oregeorev.2019.103031.
Liao, S.Y., Wang, D.B., Tang, Y., Yin, F.G., Sun, Z.M., and Sun, J., 2013, LA-ICP-MS U-Pb age of two-mica granite in the Yunlong tin-tungsten metallogenic belt in Three River region and its geological implications: Acta Petrologica et Mineralogica, v. 32, p. 450–462 (in Chinese with English abs.).
Lin, T.H., Mitchell, A.H.G., Chung, S.L., Tan, X.B., Tang, J.T., Oo, T., and Wu, F.Y., 2019a, Two parallel magmatic belts with contrasting isotopic characteristics from southern Tibet to Myanmar: Zircon U-Pb and Hf isotopic constraints: Journal of the Geological Society, London, v. 176, p. 574–587.
Lin, T.H., Mitchell, A.H.G., and Chung, S.L., 2019b, Early Cretaceous Mondaung-Lawa arc in Myanmar and its plausible correlation with Yunnan: Goldschmidt 2019, Barcelona, 2019, Poster Presentation, Abstract.
Liu, C.Z., Chung, S.L., Wu, F.Y., Zhang, C., Xu, Y., Wang, J.G., Chen, Y., and Guo, S., 2016a, Tethyan suturing in Southeast Asia: Zircon U-Pb and Hf-O isotopic constraints from Myanmar ophiolites: Geology, v. 44, p. 311–314.
Liu, C.Z., Zhang, C., Xu, Y., Wang, J.G., Chen, Y., Guo, S., Wu, F.Y., and Sein, K., 2016b, Petrology and geochemistry of mantle peridotites from the Kalaymyo and Myitkyina ophiolites (Myanmar): Implications for tectonic settings: Lithos, v. 264, p. 495–508.
Liu, L., Hu, R.Z., Zhong, H., Yang, J.H., Kang, L.F., Zhang, X.C., Fu, Y.Z., Mao, W., and Tang, Y.W., 2020, Petrogenesis of multistage S-type granites from the Malay Peninsula in the Southeast Asian tin belt and their relationship to Tethyan evolution: Gondwana Research, v. 84, p. 20–37.
Liu, P., Mao, J., Santosh, M., Xu, L., Zhang, R., and Jia, L., 2018, The Xiling Sn deposit, Eastern Guangdong Province, Southeast China: A new genetic model from $^{40}Ar/^{39}Ar$ muscovite and U-Pb cassiterite and zircon geochronology: Economic Geology, v. 113, p. 511–530.
Liu, Y.S., Hu, Z.C., Gao, S., Günther, D., Xu, J., Gao, C.G., and Chen, H.H., 2008, In situ analysis of major and trace elements of anhydrous minerals by LA-ICP-MS without applying an internal standard: Chemical Geology, v. 257, p. 34–43.
Liu, Y.S., Hu, Z.C., Zong, K.Q., Gao, C.G., Gao, S., Xu, J., and Chen, H.H., 2010, Reappraisement and refinement of zircon U-Pb isotope and trace element analyses by LA-ICP-MS: Chinese Science Bulletin, v. 55, p. 1535–1546.
Ludwig, K.R., 2003, User's manual for Isoplot/Ex., version 3.00: A geochronological toolkit for Microsoft Excel: Berkeley, California, Berkeley Geochronology Center Special Publication, p. 1–70.
Ma, N., 2014, Magmatism and mineralization in the Tengchong tin-polymetallic metallogenic belt: Ph.D. thesis, Beijing, China University of Geosciences (Beijing), 172 p. (in Chinese with English abs.).
Mao, J.W., Xie, G.Q., Guo, C.L., and Chen, Y.C., 2007, Large-scale tungsten-tin mineralization in the Nanling region, South China: Metallogenic ages and corresponding geodynamic processes: Acta Petrologica Sinica, v. 23, p. 2329–2338 (in Chinese with English abs.).
Mao, J.W., Cheng, Y.B., Chen, M.H., and Pirajno, F., 2013, Major types and time-space distribution of Mesozoic ore deposits in South China and their geodynamic settings: Mineralium Deposita, v. 48, p. 267–294.
Mao, W., Zhong, H., Yang, J.H., Tang, Y.W., Liu, L., Fu, Y.Z., Zhang, X.C., Sein, K., Aung, S.M., Li, J., and Zhang, L., 2020, Combined zircon, molybdenite, and cassiterite geochronology and cassiterite geochemistry of the Kuntabin tin-tungsten deposit in Myanmar: Economic Geology, v. 115, p. 581–601.
Metcalfe, I., 1984, Stratigraphy, palaeontology and palaeogeography of the Carboniferous of Southeast Asia: Memoires de la Societe Geographique de France, v. 147, p. 107–118.
——1996, Pre-Cretaceous evolution of SE Asian terranes: Geological Society, London, Special Publication 106, p. 97–122.
——2011, Palaeozoic-Mesozoic history of SE Asia: Geological Society, London, Special Publication 355, p. 7–35.
——2013, Gondwana dispersion and Asian accretion: Tectonic and palaeogeographic evolution of eastern Tethys: Journal of Asian Earth Sciences, v. 66, p. 1–33.
——2021, Multiple Tethyan ocean basins and orogenic belts in Asia: Gondwana Research, doi: 10.1016/j.gr.2021.01.012.
Mitchell, A.H.G., 1977, Tectonic settings for emplacement of Southeast Asian tin granites: Bulletin of the Geological Society of Malaysia, v. 9, p. 123–140.
——1979, Rift-, subduction- and collision-related tin belts: Bulletin of the Geological Society of Malaysia, v. 11, p. 81–102.
——1986, Mesozoic and Cenozoic regional tectonics and metallogenesis in Mainland SE Asia: Bulletin of the Geological Society of Malaysia, v. 20, p. 221–239.

——1993, Cretaceous-Cenozoic tectonic events in the western Myanmar (Burma)-Assam region: Journal of the Geological Society, London, v. 150, p. 1809–1102.
——2018, Geological belts, plate boundaries, and mineral deposits in Myanmar: Amsterdam, Netherlands, Elsevier, 509 p.
Mitchell, A.H.G., and Garson, M.S., 1981, Mineral deposits and global tectonic settings: London, Academic Press, 405 p.
Mitchell, A.H.G., Myint, W., Lynn, K., Htay, M.T., Oo, M., and Zaw, T., 2011, Geology of the high sulfidation copper deposits, Monywa mine, Myanmar: Resource Geology, v. 61, p. 1–29.
Mitchell, A.H.G., Chung, S.L., Oo, T., Lin, T.H., and Hung, C.H., 2012, Zircon U-Pb ages in Myanmar: Magmatic-metamorphic events and the closure of a Neo-Tethys ocean?: Journal of Asian Earth Sciences, v. 56, p. 1–23.
Mitchell, A.H.G., Htay, M.T., and Htun, K.M., 2015, The medial Myanmar suture zone and the Western Myanmar-Mogok foreland: Journal of Myanmar Geosciences Society, v. 6, p. 73–88.
Mitchell, A.H.G., Htun, K.M., and Htay, M.T., 2020a, Mondaung-Lawa and Popa-Loimye arcs and other belts, their mineral deposits and other settings: Myanmar Geosciences Society, International Congress on Geosciences of Myanmar and Surrounding Regions, 4th, Yangon, 2020, Abstracts, p. 5–7.
Mitchell, A.H.G., Htun, K.M., Htay, M.T., and Lin, T.H., 2020b, Post-Triassic Myanmar west of the Salween: Three crustal blocks, two arcs and the Mogok metamorphic belt: Journal of the Myanmar Geological Society, v. 9, p. 71–84.
Mitchell, A.H.G., Htay, M.T., and Htun, K.M., 2021, Middle Jurassic arc reversal, Victoria-Katha block and Sibumasu terrane collision, jadeite formation and Western tin belt generation, Myanmar: Geological Magazine, v. 158, p. 1487–1503.
Moscati, R.J., and Neymark, L.A., 2020, U-Pb geochronology of tin deposits associated with the Cornubian batholith of southwest England: Direct dating of cassiterite by in situ LA-ICPMS: Mineralium Deposita, v. 55, p. 1–20.
Myanmar Geosciences Society, 2014, Geological map of Myanmar: Yangon, Myanmar, scale 1:2,250,000.
Myint, A.Z., Zaw, K., Swe, Y.M., Yonezu, K., Cai, Y., Manaka, T., and Watanabe, K., 2017, Geochemistry and geochronology of granites hosting the Mawchi Sn-W deposit, Myanmar: Implications for tectonic setting and emplacement: Geological Society, London, Memoirs, v. 48, p. 385–400.
Myint, A.Z., Yonezu, K., Boyce, A.J., Selby, D., Scherstén, A., Tindell, T., Watanabe, K., and Swe, Y.M., 2018, Stable isotope and geochronological study of the Mawchi Sn-W deposit, Myanmar: Implications for timing of mineralization and ore genesis: Ore Geology Reviews, v. 95, p. 663–679.
Myint, A.Z., Li, H., Mitchell, A., Selby, D., and Wagner, T., 2021, Geology, mineralogy, ore paragenesis, and molybdenite Re-Os geochronology of Sn-W (-Mo) mineralization in Padatgyaung and Dawei, Myanmar: Implications for timing of mineralization and tectonic setting: Journal of Asian Earth Sciences, v. 212, doi: 10.1016/j.jseaes.2021.104725.
Neymark, L.A., Holm-Denoma, C.S., and Moscati, R.J., 2018, In situ LA-ICPMS U-Pb dating of cassiterite without a known-age matrix-matched reference material: Examples from worldwide tin deposits spanning the Proterozoic to the Tertiary: Chemical Geology, v. 483, p. 410–425.
Neymark, L.A., Holm-Denoma, C.S., Larin, A.M., Moscati, R.J., and Plotkina, Y.V., 2021, LA-ICPMS U-Pb dating reveals cassiterite inheritance in the Yazov granite, eastern Siberia: Implications for tin mineralization: Mineralium Deposita, doi: 10.1007/s00126-020-01038-9.
Ng, S.W.P., Whitehouse, M.J., Searle, M.P., Robb, L.J., Ghani, A.A., Chung, S.L., Oliver, G.J.H., Sone, M., Gardiner, N.J., and Roselee, M.H., 2015, Petrogenesis of Malaysian granitoids in the Southeast Asian tin belt: Part 2. U-Pb zircon geochronology and tectonic model: Geological Society of America Bulletin, v. 127, p. 1238–1258.
Paik, M., 2017, Geochemistry and geochronology of granitoid rocks in the Mawpalaw Taung area, Thanbyuzayat Township, southern Myanmar: Their petrogenesis and tectonic setting: Geological Society, London, Memoirs, v. 48, p. 401–412.
Penzer, N.M., 1922, The mineral resources of Burma: London, George Routledge and Sons, 177 p.
Qiu, Z., Li, S., Yan, Q., Wang, H., Wei, X., Li, P., Wang, L., and Bu, A., 2017, Late Jurassic Sn metallogeny in eastern Guangdong, SE China coast: Evidence from geochronology, geochemistry and Sr-Nd-Hf-S isotopes of the Dadaoshan Sn deposit: Ore Geology Reviews, v. 83, p. 63–83.
Rainbird, R.H., Heaman, L.M., and Young, G., 1992, Sampling Laurentia: Detritai zircon geochronology offers evidence for an extensive Neoproterozoic river system originating from the Grenville orogen: Geology, v. 20, p. 351–354.
Ridd, M.F., 2016, Should Sibumasu be renamed Sibuma? The case for a discrete Gondwana-derived block embracing western Myanmar, upper Peninsular Thailand and NE Sumatra: Journal of the Geological Society, London, v. 173, p. 249–264.
——2017, The Karen-Tenasserim unit: Geological Society, London, Memoirs, v. 48, p. 365–384.
Ridd, M.F., Barber, A.J., and Crow, M.J., 2011, The geology of Thailand: London, Geological Society of London, p. 1–626.
Ridd, M.F., Crow, M.J., and Morley, C.K., 2019, The role of strike-slip faulting in the history of the Hukawng block and the Jade Mines uplift, Myanmar: Proceedings of the Geologists' Association, v. 130, p. 126–141.
Rizvanova, N.G., and Kuznetsov, A.B., 2020, A new approach to ID-TIMS U-Pb dating of cassiterite by the example of the Pitkäranta tin deposit: Doklady Earth Sciences, v. 491, p. 146–149.
Romer, R.L., 2003, Alpha-recoil in U-Pb geochronology: Effective sample size matters: Contributions to Mineralogy and Petrology, v. 145, p. 481–491.
Romer, R.L., and Kroner, U., 2016, Phanerozoic tin and tungsten mineralization—tectonic controls on the distribution of enriched protoliths and heat sources for crustal melting: Gondwana Research, v. 31, p. 60–95.
Romer, R.L., Thomas, R., Stein, H.J., and Rhede, D., 2007, Dating multiply overprinted Sn-mineralized granites—examples from the Erzgebirge, Germany: Mineralium Deposita, v. 42, p. 337–359.
Royden, L.H., Burchfiel, B.C., and van der Hilst, R.D., 2008, The geological evolution of the Tibetan Plateau: Science, v. 231, p. 1054–1058.
Rudnick, R.L., and Gao, S., 2014, Composition of the continental crust, *in* Holland, H.D., and Turekian, K.K., eds, Treatise on geochemistry, v. 3: Amsterdam, Elsevier, p. 1–51.
Sainsbury, C.L., 1969, Tin resources of the world: U.S. Geological Survey, Bulletin 1301, p. 1–55, https://pubs.usgs.gov/bul/1301/report.pdf.
Sanematsu, K., Manaka, T., and Zaw, K., 2014, Geochemical and geochronological charactersistics of granites and Sn-W-REE mineralisation in the Tanintharyi region, southern Myanmar: Myanmar Geosciences Society, Regional Congress on Geology, Mineral and Energy Resources of Southeast Asia, Yangon, 2014, Abstracts, p. 77–102.
Schuiling, R.D., 1967, Tin belts on the continents around the Atlantic Ocean: Economic Geology, v. 62, p. 540–550.
Schulz, K.J., DeYoung, J.H., Jr., R.R.S.I., and Bradley, D.C., 2017, Critical mineral resources of the United States—economic and environmental geology and prospects for future supply: U.S. Geological Survey, Professional Paper 1802, p. 1–797.
Schwartz, M.O., Rajah, S.S., Askury, A., Putthapiban, P., and Djaswadi, S., 1995, The Southeast Asian tin belt: Earth-Science Reviews, v. 38, p. 95–263.
Searle, M.P., Noble, S.R., Cottle, J.M., Waters, D.J., Mitchell, A.H.G., Hlaing, T., and Horstwood, M.S.A., 2007, Tectonic evolution of the Mogok metamorphic belt, Burma (Myanmar) constrained by U-Th-Pb dating of metamorphic and magmatic rocks: Tectonics, v. 26, doi: 10.1029/2006TC002083.
Searle, M.P., Whitehouse, M.J., Robb, L.J., Ghani, A.A., Hutchison, C.S., Sone, M., Ng, S.W.P., Roselee, M.H., Chung, S.L., and Oliver, G.J.H., 2012, Tectonic evolution of the Sibumasu-Indochina terrane collision zone in Thailand and Malaysia: Constraints from new U-Pb zircon chronology of SE Asian tin granitoids: Journal of the Geological Society, London, v. 169, p. 489–500.
Searle, M.P., Robb, L.J., and Gardiner, N.J., 2016, Tectonic processes and metallogeny along the Tethyan mountain ranges of the Middle East and South Asia (Oman, Himalaya, Karakoram, Tibet, Myanmar, Thailand, Malaysia): Society of Economic Geologists, Special Publication 19, p. 301–327.
Sengör, A.M.C., Altmer, D., Cin, A., Ustaomer, T., and Hsu, K.J., 1988, Origin and assembly of the Tethyside orogenic collage at the expense of Gondwana Land: Geological Society of London, Special Publication 37, p. 119–181.
Sillitoe, R.H., 2012, Copper provinces: Society of Economic Geologists, Special Publication 16, p. 1–18.
Sláma, J., Košler, J., Condon, D.J., Crowley, J.L., Gerdes, A., Hanchar, J.M., Horstwood, M.S.A., Morris, G.A., Nasdala, L., Norberg, N., et al., 2008, Plešovice zircon—a new natural reference material for U-Pb and Hf isotopic microanalysis: Chemical Geology, v. 249, p. 1–35.
Smoliar, M.I., Walker, R.J., and Morgan, J.W., 1996, Re-Os ages of group IIA, IIIA, IVA, and IVB iron meteorites: Science, v. 271, p. 1099–1102.
Solomon, M., and Groves, D.I., 1994, The geology and origin of Australia's mineral deposits: London, Oxford Science Publications, 951 p.
Sone, M., and Metcalfe, I., 2008, Parallel Tethyan sutures in mainland Southeast Asia: New insights for Palaeo-Tethys closure and implications for the Indosinian orogeny: Comptes Rendus Geoscience, v. 340, p. 166–179.

Tang, Y., Cui, K., Zheng, Z., Gao, J., Han, J., Yang, J., and Liu, L., 2020, LA-ICP-MS U-Pb geochronology of wolframite by combining NIST series and common lead-bearing MTM as the primary reference material: Implications for metallogenesis of South China: Gondwana Research, v. 83, p. 217–231.

Tapponnier, P., Lacassin, R., Leloup, P.H., Schärer, U., Zhong, D.L., Liu, X.H., Ji, S.C., Zhang, L.S., and Zhong, J.Y., 1990, The Ailao Shan/Red River metamorphic belt: Tertiary left-lateral shear between Indochina and South China: Nature, v. 343, p. 431–437.

Taylor, R.G., 1979, Geology of tin deposits: Academic Press, Elsevier, 543 p.

U.S. Geological Survey (USGS), 2020, Mineral commodity summaries 2020, 200 p., doi: 10.3133/mcs2020.

Wang, C., Deng, J., Carranza, E.J.M., and Santosh, M., 2014, Tin metallogenesis associated with granitoids in the southwestern Sanjiang Tethyan domain: Nature, deposit types, and tectonic setting: Gondwana Research, v. 26, p. 576–593.

Wang, C., Deng, J., Santosh, M., Lu, Y., McCuaig, T.C., Carranza, E.J.M., and Wang, Q., 2015, Age and origin of the Bulangshan and Mengsong granitoids and their significance for post-collisional tectonics in the Changning-Menglian Paleo-Tethys orogen: Journal of Asian Earth Sciences, v. 113, p. 656–676.

Wiedenbeck, M., Allé, P., Corfu, F., Griffin, W.L., Meier, M., Oberli, F., von Quadt, A., Roddick, J.C., and Spiegel, W., 1995, Three natural zircon standards for U-Th-Pb, Lu-Hf, trace element and REE analyses: Geostandards Newsletter, v. 19, p. 1–23.

Xie, J.C., Zhu, D.C., Dong, G., Zhao, Z.D., Wang, Q., and Mo, X., 2016, Linking the Tengchong terrane in SW Yunnan with the Lhasa terrane in southern Tibet through magmatic correlation: Gondwana Research, v. 39, p. 217–229.

Xu, Z., Wang, Q., Cai, Z., Dong, H., Li, H., Chen, X., Duan, X., Cao, H., Li, J., and Burg, J.P., 2015, Kinematics of the Tengchong terrane in SE Tibet from the late Eocene to early Miocene: Insights from coeval mid-crustal detachments and strike-slip shear zones: Tectonophysics, v. 665, p. 127–148.

Yang, J.H., Zhou, M.F., Hu, R.Z., Zhong, H., Williams-Jones, A.E., Liu, L., Zhang, X.C., Fu, Y.Z., and Mao, W., 2020, Granite-related tin metallogenic events and key controlling factors in Peninsular Malaysia, Southeast Asia: New insights from cassiterite U-Pb dating and zircon geochemistry: Economic Geology, v. 115, p. 581–601.

Yang, M., Yang, Y.H., Wu, S.T., Romer, R.L., Che, X.D., Zhao, Z.F., Li, W.S., Yang, J.H., Wu, F.Y., Xie, L.W., Huang, C., Zhang, D., and Zhang, Y., 2020, Accurate and precise in situ U-Pb isotope dating of wolframite series minerals via LA-SF-ICP-MS: Journal of Analytical Atomic Spectrometry, v. 35, p. 2191–2203.

Yu, L., Li, G.J., Wang, Q.F., and Liu, X.F., 2014, Petrogenesis and tectonic significance of the Late Cretaceous magmatism in the northern part of the Baoshan block: Constraints from bulk geochemistry, zircon U-Pb geochronology and Hf isotope compositions: Acta Petrologica Sinica, v. 30, p. 2709–2724 (in Chinese with English abs.).

Yuan, S.D., Peng, J.T., Hao, S., Li, H.M., Geng, J.Z., and Zhang, D.L., 2008, A precise U-Pb age on cassiterite from the Xianghualing tin-polymetallic deposit (Hunan, South China): Mineralium Deposita, v. 43, p. 375–382.

Yuan, S.D., Peng, J.T., Hu, R.Z., Li, H.M., Shen, N.P., and Zhang, D.L., 2011, In situ LA-MC-ICP-MS and ID-TIMS U-Pb geochronology of cassiterite in the giant Furong tin deposit, Hunan Province, South China: New constraints on the timing of tin-polymetallic mineralization: Ore Geology Reviews, v. 43, p. 235–242.

Zaw, K., 1990, Geological, petrological and geochemical characteristics of granitoid rocks in Burma: With special reference to the associated W-Sn mineralization and their tectonic setting: Journal of Southeast Asian Earth Sciences, v. 4, p. 293–335.

——2017, Overview of mineralization styles and tectonic-metallogenic setting in Myanmar: Geological Society, London, Memoirs, v. 48, p. 531–556.

Zhang, D.L., Peng, J.T., Hu, R.Z., Yuan, S.D., and Zheng, D.S., 2011, The closure of U-Pb isotope system in cassiterite and its reliability for dating: Geological Review, v. 57, p. 549–554 (in Chinese with English abs.).

Zhang, R., Lehmann, B., Seltmann, R., Sun, W., and Li, C., 2017a, Cassiterite U-Pb geochronology constrains magmatic-hydrothermal evolution in complex evolved granite systems: The classic Erzgebirge tin province (Saxony and Bohemia): Geology, v. 45, p. 1095–1098.

Zhang, R., Sun, W., Li, C., Lehmann, B., and Seltmann, R., 2017b, Constraints on tin mineralization events by cassiterite LA-ICP-MS U-Pb dating: Society for Geology Applied to Mineral Deposits (SGA), Biennial Meeting, 14th, Quebec City, Canada, August 20–23, Proceedings, v. 3, p. 1009–1012.

Zhang, S., Zhang, R., Lu, J., Ma, D., Ding, T., Gao, S., and Zhang, Q., 2019, Neoproterozoic tin mineralization in South China: Geology and cassiterite U-Pb age of the Baotan tin deposit in northern Guangxi: Mineralium Deposita, v. 54, p. 1125–1142.

Zhou, X.P., Qi, H.W., Hu, R.Z., Bi, X.W., and Meng, Y.M., 2015, Geochronology and geochemistry of granites in the Tengchong Xinqi area, western Yunnan and their tectonic implication: Bulletin of Mineralogy, Petrology and Geochemistry, v. 34, p. 139–147 (in Chinese with English abs.).

Zhou, X.P., Qi, H.W., Qu, W.J., and Li, C., 2017, Re-Os isotopic dating for molybdenites in Xinqi tungsten-tin polymetallic deposit of Yunnan Province, China and its geological significance: Acta Mineralogica Sinica, v. 37, p. 84–92 (in Chinese with English abs.).

Wei Mao is an associate professor at the Institute of Geochemistry, Chinese Academy of Sciences. He obtained his B.S. degree in geology from Northwest University in 2011 and a Ph.D. degree in economic geology from the University of Chinese Academy of Sciences in 2016. His current research interest is in metal transportation, enrichment, and precipitation processes in magmatic-hydrothermal systems, especially in porphyry Cu-Mo deposits and granite-related Sn-W deposits in South China and Southeast Asia.